

Search for long-lived heavy neutral leptons decaying in the CMS muon detectors in proton-proton collisions at $\sqrt{s} = 13$ TeV

CMS Collaboration; Bols, Emil Sørensen; D'Hondt, Jorgen; Dansana, Soumya; De Moor, Alexandre; Delcourt, Martin; El Faham, Hesham; Lowette, Steven; Makarenko, Inna; Müller, Denise; Sahasransu, Abanti Ranadhir; Tavernier, Stefaan; Tytgat, Michael; Van Putte, Senne; Vannerom, David; Stylianou, Nicolas

Published in:
Physical Review D

DOI:
[10.1103/PhysRevD.110.012004](https://doi.org/10.1103/PhysRevD.110.012004)

Publication date:
2024

License:
CC BY

Document Version:
Final published version

[Link to publication](#)

Citation for published version (APA):

CMS Collaboration, Bols, E. S., D'Hondt, J., Dansana, S., De Moor, A., Delcourt, M., El Faham, H., Lowette, S., Makarenko, I., Müller, D., Sahasransu, A. R., Tavernier, S., Tytgat, M., Van Putte, S., Vannerom, D., & Stylianou, N. (2024). Search for long-lived heavy neutral leptons decaying in the CMS muon detectors in proton-proton collisions at $\sqrt{s} = 13$ TeV. *Physical Review D*, *110*(1), Article 012004. <https://doi.org/10.1103/PhysRevD.110.012004>

Copyright

No part of this publication may be reproduced or transmitted in any form, without the prior written permission of the author(s) or other rights holders to whom publication rights have been transferred, unless permitted by a license attached to the publication (a Creative Commons license or other), or unless exceptions to copyright law apply.

Take down policy

If you believe that this document infringes your copyright or other rights, please contact openaccess@vub.be, with details of the nature of the infringement. We will investigate the claim and if justified, we will take the appropriate steps.

Search for long-lived heavy neutral leptons decaying in the CMS muon detectors in proton-proton collisions at $\sqrt{s} = 13$ TeV

A. Hayrapetyan *et al.**
(CMS Collaboration)

 (Received 28 February 2024; accepted 8 May 2024; published 8 July 2024)

A search for heavy neutral leptons (HNLs) decaying in the CMS muon system is presented. A data sample is used corresponding to an integrated luminosity of 138 fb^{-1} of proton-proton collisions at $\sqrt{s} = 13$ TeV, recorded at the CERN LHC in 2016–2018. Decay products of long-lived HNLs could interact with the shielding materials in the CMS muon system and create hadronic and electromagnetic showers detected in the muon chambers. This distinctive signature provides a unique handle to search for HNLs with masses below 4 GeV and proper decay lengths of the order of meters. The signature is sensitive to HNL couplings to all three generations of leptons. Candidate events are required to contain a prompt electron or muon originating from a vertex on the beam axis and a displaced shower in the muon chambers. No significant deviations from the standard model background expectation are observed. In the electron (muon) channel, the most stringent limits to date are set for HNLs in the mass range of 2.1–3.0 (1.9–3.3) GeV, reaching mixing matrix element squared values as low as $8.6(4.6) \times 10^{-6}$.

DOI: [10.1103/PhysRevD.110.012004](https://doi.org/10.1103/PhysRevD.110.012004)

I. INTRODUCTION

The observation of neutrino oscillations [1–3] provides experimental evidence for nonzero neutrino masses [4]. Cosmological considerations [5,6] and direct measurements [7] imply that the neutrino masses are much smaller than both the masses of other standard model (SM) fermions and the vacuum expectation value of the Higgs field, hinting at a different mechanism for generating masses of neutrinos compared with that for the masses of charged fermions.

One possible explanation of the nonzero neutrino masses is the existence of heavy neutral leptons (HNLs) with right-handed chirality, giving rise to the gauge-invariant mass terms for the SM neutrinos through the “seesaw” mechanism [8–15]. The HNLs are singlets with respect to the SM gauge groups and therefore do not interact with SM particles through the electroweak or strong interactions, but can be produced through mixing with the SM electron, muon, and τ neutrinos [16–20]. There can be either distinct HNL particles and antiparticles [(pseudo-)Dirac type], or the HNL can be its own antiparticle (Majorana type). An HNL is characterized by its mass m_N and its mixing matrix elements $V_{N\ell}$, with $\ell = e, \mu, \tau$, respectively. The HNL

lifetime is inversely proportional to $m_N^5 |V_{N\ell}|^2$ [21], and HNLs can be macroscopically long-lived for sufficiently low values of mixing matrix elements. Models with HNLs are well motivated because they can explain the baryon asymmetry of the Universe through CP violation in the HNL system [22,23], provide a dark matter candidate [24], and explain the observed anomalous magnetic moment of the muon [25,26].

Past searches for HNLs have covered a wide range of masses ranging from a few keV to several TeV [27–33]. At the CERN LHC, searches conducted by the ATLAS, CMS, and LHCb Collaborations [34–40] have targeted both prompt and long-lived HNL decays. The search presented in this paper focuses on HNLs with masses between 1 and 4 GeV. In this region, the most stringent prior limits for the muon (electron) mixing parameter $|V_{N\mu}|^2$ ($|V_{Ne}|^2$) have been set by the BEBC, CHARM, and NuTeV experiments [27,28,30] below about 1.9 (2.1) GeV and by the CMS searches [38,41] for masses above 1.9 (2.1) GeV. The most stringent prior limits for the τ mixing parameter $|V_{N\tau}|^2$ have been set by the DELPHI and CHARM experiments [28,29]. This search aims to extend the discovery reach toward the lowest values of $|V_{N\ell}|^2$ achieved in the 1–4 GeV mass range.

In this paper, a search for Dirac and Majorana HNLs with mean proper decay lengths ($c\tau_0$) in the range of 0.1–10 m is performed. A data sample collected by the CMS experiment in 2016–2018 and corresponding to an integrated luminosity of 138 fb^{-1} is used. An HNL that decays via a virtual W boson can result in a final state with two charged leptons and a neutrino, or one lepton and two quarks.

*Full author list given at the end of the article.

Published by the American Physical Society under the terms of the [Creative Commons Attribution 4.0 International license](https://creativecommons.org/licenses/by/4.0/). Further distribution of this work must maintain attribution to the author(s) and the published article's title, journal citation, and DOI. Funded by SCOAP³.

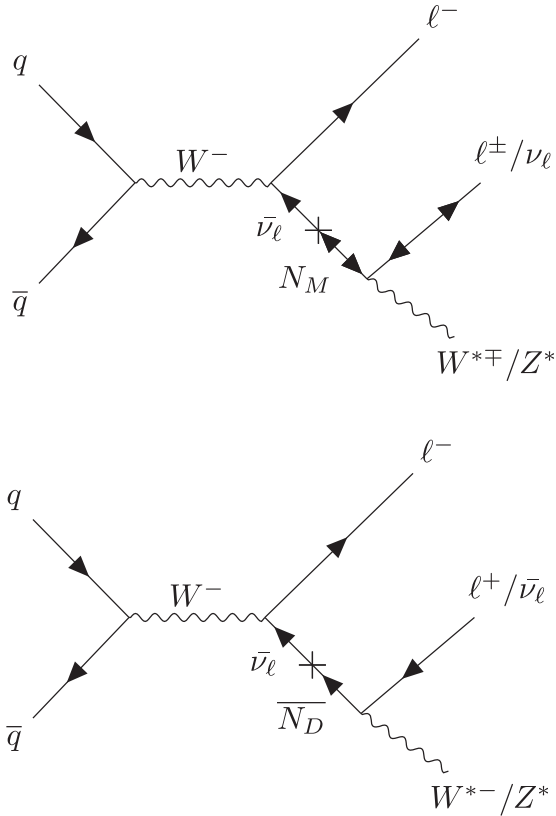


FIG. 1. Feynman diagrams for the production of a Majorana HNL N_M (upper) and a Dirac HNL N_D (lower) via a W^- boson decay and through its mixing with an SM neutrino of the same flavor. The prompt lepton from the W^- boson serves as a clean signature for triggering, whereas the decay products of the HNL are reconstructed as a cluster of muon detector hits.

Figure 1 shows the Feynman diagram for the production of an HNL via W boson decay, where the prompt lepton from the W boson decay originates from a vertex on the beam axis and serves as a clean signature for triggering. We search for HNL decays occurring within the muon detector system. The hadrons and electrons from the HNL decays, including those resulting from an intermediate τ lepton, could produce a particle shower as they interact with the steel shielding material of the muon detectors. This process results in the striking signature of a localized high-multiplicity cluster of muon detector hits, referred to as a muon detector shower (MDS) object. Because of the macroscopic distance from the primary interaction point to the muon detectors and its large volume of geometric acceptance, this signature is sensitive to a large class of models involving long-lived particles (LLPs). It is uniquely sensitive to HNLs with $c\tau_0$ in the range 0.1–10 m, extending the search sensitivity to unprecedentedly low mixing parameter values in the m_N range of 1–3 GeV. We follow an analysis strategy for MDS objects that is similar to one used by CMS in Ref. [42].

The outline of the paper is as follows: a brief description of the CMS detector is given in Sec. II. The dataset and the

simulated samples of events are detailed in Sec. III, followed by a description of the event selection and categorization in Sec. IV. A description of the backgrounds and the method used to estimate them is given in Sec. V. Sources of systematic uncertainty affecting the expected numbers of signal and background events are discussed in Sec. VI. The results and their interpretations are presented in Sec. VII, followed by a summary of the paper in Sec. VIII. The numerical results of this paper can be found in its HEPData [43] record.

II. THE CMS DETECTOR

The central feature of the CMS detector is a superconducting solenoid of 6 m internal diameter, providing a magnetic field of 3.8 T. Within the solenoid volume are a silicon pixel and strip tracker, a lead tungstate crystal electromagnetic calorimeter (ECAL), and a brass and scintillator hadron calorimeter (HCAL), each composed of a barrel and two end cap sections. The ECAL consists of 75,848 lead tungstate crystals, which cover $|\eta| < 1.48$ in the barrel region and $1.48 < |\eta| < 3.00$ in the two end cap regions. The HCAL is composed of cells of width 0.087 in η and azimuth (ϕ , in radians) for the region $|\eta| < 1.74$, progressively increasing to a maximum of 0.174 for larger values of $|\eta|$, along with the forward calorimeters extending the η coverage provided by the barrel and end cap detectors.

Muons are measured in the pseudorapidity range of $|\eta| < 2.4$, with detection planes embedded in the steel flux-return yoke outside the solenoid and made using three technologies: drift tubes (DTs), cathode strip chambers (CSCs), and resistive-plate chambers (RPCs).

The barrel DT detectors cover $|\eta| < 1.2$ and are organized into four layers (“stations”), labeled MB1–MB4. The stations are located approximately 4–7 m in radial distance (r) from the interaction point. Each station is a concentric ring of chambers, interleaved with the layers of the steel flux-return yoke of the solenoid and is divided along the beamline axis (z) into five wheels. In the first three stations, every DT chamber consists of three “superlayers” (SLs), each comprising four staggered layers of parallel DT cells, for a total of 12 layers. The innermost and outermost SLs measure the hit coordinate in the $r\phi$ plane, and the central SL measures in the z direction, along the beamline. The fourth station (MB4) contains only two SLs measuring the hit position in the $r\phi$ plane. The DT cells are designed to provide a uniform electric field, such that the position of a traversing charged particle can be inferred from the measured arrival time and the constant drift velocity. Individual hits have a resolution of about 600 μm which can be improved to about 260 μm by incorporating information from hits in the same SL [44].

The CSC detectors cover $0.9 < |\eta| < 2.4$ and comprise four stations in each end cap, labeled ME1–ME4. Each station is a ring of chambers interleaved between two layers of steel flux-return yoke at approximately the same value

of z . The stations are located approximately 7, 8, 9.5, and 10.5 m from the interaction point along the beamline axis on both ends of the detector. Each chamber consists of six layers containing cathode strips along the radial direction and anode wires perpendicular to the central strip. Position and timing measurements of traversing charged particles are extracted from the electrical signals on the anode wires and the cathode strips in each chamber, for which the typical resolutions are 400–500 μm and 5 ns.

The RPC detectors are placed alongside the DT and CSC detectors and are primarily designed to provide timing information for the muon trigger.

Events of interest are selected using a two-tiered trigger system. The first level, composed of custom hardware processors, uses information from the calorimeters and muon detectors to select events at a rate of around 100 kHz within a fixed latency of about 4 μs [45]. The second level, known as the high-level trigger, consists of a farm of processors running a version of the full event reconstruction software optimized for fast processing and reduces the event rate to around 1 kHz before data storage [46]. A more detailed description of the CMS detector, together with a definition of the coordinate system used and the relevant kinematic variables, is reported in Ref. [47].

III. SIMULATED SAMPLES

Simulated samples of Drell-Yan produced $Z + \text{jets}$ are used to validate the MDS object reconstruction efficiency. They are produced using POWHEG 2.0 [48–50] and normalized to next-to-next-to-leading-order (NNLO) precision [51,52]. Signal samples for HNL production are generated at leading order with the Monte Carlo (MC) generator MadGraph5_aMC@NLO 2.3.3 [53–56]. This matrix element level calculation includes only the W -channel production of HNLs with up to two additional partons. The simulated events are interfaced with PYTHIA 8.226 [57] to simulate the parton shower and hadronization of partons and the underlying event description.

The branching fraction of W boson decays into an HNL plus a lepton is proportional to the mixing parameter $|V_{N\ell}|^2$. The signatures considered in this search are sensitive to mixing with ν_e , ν_μ , or ν_τ since the decay products of the HNL in the muon detector system are reconstructed as particle showers. The final states consist of one prompt lepton (e or μ) from the W boson decay and HNL decay products. To account for higher order effects, the cross sections of the signal samples are scaled to the NNLO W boson production cross section, which is 20510 ± 770 pb [58] including the branching fraction to one lepton flavor, multiplied by the square of the HNL mixing matrix elements. The branching ratios to all three lepton generations are assumed to be the same. To obtain a more accurate description of the boost of the HNL signal,

W -boson- p_T -dependent corrections based on an MC sample generated with DYTurbo1.3.2 at next-to-next-to-next-to-leading-logarithm and next-to-NNLO accuracy [59,60] are computed and applied as an event-by-event weight.

Signals corresponding to both Dirac and Majorana HNLs are considered in this search, for $c\tau_0$ values in the range of 0.1–10 m. Lepton number violating (LNV) decays are only possible for Majorana HNLs, whereas lepton number conserving (LNC) decay channels are available for both Majorana and Dirac HNLs. This distinction implies that the widths of the Dirac HNL are exactly half of that of the Majorana HNLs for the same m_N and mixing matrix; therefore, the lifetime of the Dirac HNLs will be twice the Majorana ones [56]. In this search, the charged lepton from the HNL decay is either not detected or its charge is not measured, resulting in identical detector response between LNV and LNC events. Therefore, we can predict the signal yields of a simulated Majorana sample as those from a Dirac HNL sample with twice the lifetime.

Generated events are processed through a simulation of the detector geometry and response using Geant4 [61]. The same reconstruction software is applied to both data and simulated events. Simulated events include an expected distribution of the number of additional pp interactions within the same or nearby bunch crossings (pileup). All generated events are weighted such that the distribution of the number of collisions per bunch crossing matches the one observed in data, with an average of approximately 23 (32) interactions per bunch crossing [62–64] in 2016 (2017–2018). The underlying PYTHIA event tune CUETP8M1 [65] (CP5 [66]) and NNPDF3.0 [67] (3.1 [68]) parton distribution functions are used to simulate all samples for the 2016 (2017–2018) data-taking period.

The HNL signal samples are generated for m_N in the range from 1 to 4 GeV and $c\tau_0$ in the range from 0.1 to 10 m. Since only a discrete set of lifetimes was generated, the signal predictions for intermediate lifetimes were estimated by performing the reweighting procedure described below. The simulated HNLs are assumed to couple exclusively to one of the three SM neutrino families. The signal production cross sections and lifetimes are determined by the values of m_N and $|V_{N\ell}|^2$, which in turn determine the signal acceptance and reconstruction efficiency. Thus, for a fixed value of m_N , a simple cross section rescaling is not sufficient to correctly reproduce the behavior of other HNLs with the same m_N but different $|V_{N\ell}|^2$. To emulate an HNL signal sample with a specific value of $|V_{N\ell}|^2$ (and thus $c\tau_0$), we thus apply per-event weights to the events, such that the HNL lifetime distribution (taken before the parton shower and detector simulation) matches the predicted distribution for the chosen $|V_{N\ell}|^2$ value. For signal scenarios with m_N between the masses of the simulated samples, we estimate the signal yield by interpolating between the predictions from the simulated samples at nearby m_N using the fact that the

acceptance of the muon system differs only through the Lorentz boost factor.

IV. EVENT RECONSTRUCTION AND SELECTION

The objects in each event are reconstructed using the particle-flow (PF) algorithm [69], which aims to identify each individual particle in an event as an electron, photon, muon, charged or neutral hadron, with an optimized combination of information from the various elements of the CMS detector. The resulting particles are referred to as PF candidates. Each electron is identified as a charged-particle track that extrapolates to an ECAL energy cluster and any nearby ECAL clusters that are consistent with possible bremsstrahlung photons [70]. The electron momentum is estimated by combining the energy measurement in the ECAL with the momentum measurement in the tracker. Muons are identified as tracks in the central tracker consistent with either tracks or several hits in the muon system and associated with calorimeter deposits compatible with the muon hypothesis [71]. Photons are identified as ECAL energy clusters not linked to the extrapolation of any charged-particle trajectory to the ECAL [72]. The energies of photons are obtained from the ECAL measurement. Charged hadrons are identified as charged-particle tracks neither identified as electrons nor as muons. The energy of each charged hadron is determined from a combination of the track momentum and the corresponding ECAL and HCAL energies, corrected for the response function of the calorimeters to hadronic showers. Finally, a neutral hadron is identified as HCAL energy clusters not linked to any charged-hadron trajectory or as a combined ECAL and HCAL energy excess with respect to the expected charged-hadron energy deposit. The energy of each neutral hadron is obtained from the corresponding corrected ECAL and HCAL energies.

To identify the electrons and muons resulting from the decays of the W bosons, we impose additional selection requirements to enhance the signal purities of these objects. For each electron candidate, requirements are imposed on the shape of the electromagnetic shower in the ECAL, the quality of the matching between the track trajectory and the ECAL shower, and isolation from additional particles near the candidate. A tight working point [70] for this electron identification is used, which has an average efficiency of 70% and a misidentification rate of about 2%. We consider electron candidates with transverse momenta $p_T > 30$ GeV and $|\eta| < 2.5$; a more stringent requirement of $p_T > 35$ GeV is imposed for the data collected in 2017–2018 to match the increase in the p_T threshold of the single electron trigger from 27 to 32 GeV. For muon candidates, requirements are imposed on the quality of the track in the silicon tracker, the global compatibility of the hits in the silicon tracker and muon detector comprising the muon candidate, and isolation from additional particles near the candidate. The tight working point [71] is used, which has

an efficiency above 95% and a misidentification rate of about 0.1% for hadrons. We consider muon candidates with $p_T > 25$ GeV and $|\eta| < 2.4$; a more stringent requirement of $p_T > 28$ GeV is imposed for the data collected in 2017 to match the increase in the p_T threshold of the single-muon trigger from 24 to 27 GeV.

In this search, jets are used to veto muon detector shower cluster objects to suppress the punchthrough jet background. Jets are reconstructed by clustering PF candidates using the anti- k_T algorithm [73,74] with a distance parameter $\Delta R = \sqrt{(\Delta\eta)^2 + (\Delta\phi)^2} = 0.4$. Jets are required to have $p_T > 10$ GeV and $|\eta| < 3.0$. Pileup can contribute additional tracks and calorimetric energy depositions to the jet momentum. To mitigate this effect, charged particles identified to be originating from pileup vertices are discarded and an offset correction is applied to account for remaining contributions [75]. Jet energy corrections are derived from simulation studies so that the average measured energy of jets becomes identical to that of particle-level jets [76].

The missing transverse momentum vector \vec{p}_T^{miss} is computed as the negative vector p_T sum of all the PF candidates in an event, and its magnitude is denoted as p_T^{miss} [77]. The jet energy corrections are propagated into the computation of p_T^{miss} . The primary vertex (PV) is taken to be the vertex corresponding to the hardest scattering in the event, evaluated using tracking information alone, as described in Sec. 9.4.1 of Ref. [78].

We select data events triggered by the single-electron or single-muon triggers and require the events to have exactly one prompt-electron or prompt-muon candidate, respectively, satisfying the identification and isolation criteria described above. To further suppress the background from SM events composed uniquely of jets produced through the strong interaction, referred to as quantum chromodynamics (QCD) multijet events, we require $p_T^{\text{miss}} > 30$ GeV. The above requirements are designed to select events with an HNL candidate produced in a W boson decay. Because the constituents of MDS clusters are not included in the p_T^{miss} calculation, typical HNL signal events would satisfy this p_T^{miss} selection.

A. Muon detector shower clusters

For LLPs that decay within or just prior to the DT and CSC muon detectors, the material in the steel flux-return yoke structure can induce a particle shower, creating a geometrically localized and isolated cluster of detector hits. In CSC chambers, the detector hits are reconstructed by combining the signal pulses from the anode wires and the cathode strips, forming a point on a two-dimensional plane in each chamber layer. In DT chambers, the detector hits are reconstructed from the signal pulses from the anode wires at the center of the DT cells. Since the DT hits only provide measurement in either the ϕ or z dimension, the DT hit

position is assumed to be at the center of each DT chamber in the orthogonal direction. Together with the position of the chambers, each CSC and DT hit is assigned a three-dimensional coordinate in space. We cluster the CSC and DT hits based on their η and ϕ coordinates using the density-based spatial clustering of applications with noise (DBSCAN) algorithm [79], which is a commonly used density-based clustering algorithm that is robust against outliers. A distance parameter of 0.2 and a minimum number of hits per cluster (N_{hits}) of 50 is used in the DBSCAN algorithm. We choose a minimum of 50 hits to avoid misidentifying a minimum ionizing muon as a cluster object. A muon is expected to produce a maximum of 24 and 44 hits in the CSC and DT detectors, respectively. The centroid of the cluster is taken to be the geometric center of the hits in the cluster. These clusters, which we refer to as MDS objects, provide a powerful signature to distinguish LLP signal events from background events.

The efficiency for MDS objects to be reconstructed depends on whether the LLP decays primarily to hadrons, including the hadronic decays of τ leptons, or to electrons and photons. Typically, more cluster hits are produced by hadrons, resulting in a higher MDS reconstruction efficiency for LLPs that decay to hadrons as compared with LLPs that decay to electrons and photons. The reconstruction efficiency is about 80 (30–45)% for hadronic (electron and photon) decays, depending on whether the MDS is reconstructed in the CSCs or DTs. Muons that are produced from HNL decays do not produce a particle shower and are not reconstructed. Further details of the efficiency dependence on LLP decay location can be found in Ref. [42].

Energetic particles produced in jet hadronization or from secondary material interactions can produce MDS clusters by traversing the shielding material between the tracking volume and the muon detectors without being stopped. To suppress this process, known as the punchthrough jet background, we veto any MDS clusters in the DT (CSC) detectors whose centroid lies within $\Delta R = 0.4$ of a jet with $p_T > 20$ (10) GeV and $|\eta| < 3.0$. To suppress clusters produced by muon bremsstrahlung, we impose a tighter veto on any MDS clusters in the DT (CSC) detectors whose centroid lies within $\Delta R = 0.8$ of a muon candidate with $p_T > 10$ (20) GeV. The p_T thresholds for the jet and muon vetoes were chosen to optimize the signal-to-background discrimination and differ between the DT and CSC detectors because of the different amounts of shielding present. Because MDS cluster hits do not enter the \vec{p}_T^{miss} calculation, the MDS cluster tends to align with the \vec{p}_T^{miss} and the momentum of the LLP in signal events. We leverage this feature to validate the background estimation method discussed in Sec. V. Muons with trajectories pointing toward two regions of the detector near the cavern chimneys have highly reduced reconstruction efficiencies

because these regions are occupied by cables and other support structures resulting in a smaller detector coverage. As a result, the rate of background MDS clusters produced by muon bremsstrahlung and passing the muon veto is significantly increased. To suppress these backgrounds, we veto any clusters whose centroid is within $\Delta R = 0.3$ of the following two locations in η and ϕ coordinates: ($\eta = 0.3$, $\phi = 1.70$) or ($\eta = -0.3$, $\phi = 1.15$), corresponding to the chimney locations.

The rate of MDS clusters caused by punchthrough jets is significantly larger for clusters with hits in the muon detector station closest to the interaction point because of the reduced amount of shielding material. Furthermore, any hits observed in the stations between the interaction point and the station containing the majority of the cluster hits are indicative of a punchthrough jet because signal LLPs are neutral and therefore do not produce any hits before they decay. To further suppress such punchthrough jets, we veto any MDS clusters in the CSCs whose centroid lies within $\Delta R = 0.4$ of any hits observed in the two innermost rings of the ME1 station (ME1/1 and ME1/2), or in the RPCs located immediately next to ME1/2, or any segments in the MB1 station. Segments are required in the MB1 station instead of single hits because of the larger rate of noise in the DT detectors, which would produce a larger signal inefficiency for such a veto. For MDS clusters in the DTs, we veto any cluster whose centroid lies within $\Delta R = 0.5$ of two or more hits in the MB1 station. We also require no more than 8 MB1 hits in the adjacent wheels within $\Delta\phi < \pi/4$. As a result of the above vetoes, only clusters located beyond the station closest to the interaction point are accepted.

After the jet and muon vetoes, the dominant background consists of clusters from pileup, including interactions not in the same bunch crossing as the PV, known as out-of-time (OOT) pileup. To eliminate the background clusters from OOT pileup, we reconstruct a characteristic time for the clusters in both the CSC and DT detectors. For the CSC clusters, the cluster time is reconstructed from the mean time of the hits comprising the cluster, where the time of each hit is calibrated to result in a distribution centered at zero for the triggering bunch crossing. Note that the adjacent bunch crossings occur at ± 25 ns with this definition. We require that the CSC cluster time ($t_{\text{cluster}}^{\text{CSC}}$) is between -5.0 and 12.5 ns and that the root-mean-square spread of the time stamps of hits comprising the cluster (t_{spread}) is less than 20 ns. Because hits in the DT detectors do not have a time measurement that is independent of their position measurement, we require that DT clusters coincide with at least one hit in an RPC detector in the same wheel and within $\Delta\phi < 0.5$ of the DT cluster centroid. The time measurements of each matching RPC hit are matched to discrete bunch crossing times. The most frequently occurring bunch crossing time among the matching RPC hits is defined as the DT cluster time ($t_{\text{cluster}}^{\text{DT}}$). The DT cluster time

is required to coincide with the bunch crossing corresponding to the PV.

Finally, additional identification requirements, developed in Ref. [42], are imposed on CSC clusters. They are required to satisfy successively more central $|\eta|$ requirements as the number of CSC stations containing hits (N_{stations}) and the distance between the station and the primary interaction point decrease. The $|\eta|$ requirements are

- (i) $|\eta| < 1.9$ if $N_{\text{stations}} > 1$,
- (ii) $|\eta| < 1.8$ if $N_{\text{stations}} = 1$ and the cluster is in station 4,
- (iii) $|\eta| < 1.6$ if $N_{\text{stations}} = 1$ and the cluster is in station 2 or station 3, and
- (iv) $|\eta| < 1.1$ if $N_{\text{stations}} = 1$ and the cluster is in station 1.

This CSC cluster identification algorithm has $\sim 60\%$ efficiency and suppresses the background by a factor of 8.

For a certain period of data taking, anomalous detector noise in specific components of the DT detectors produced a high rate of background MDS clusters. To suppress this noise-induced background, we veto MDS clusters comprising hits detected in those particular DT chambers taken during the affected time period. The amount of data rejected by this veto corresponds to less than 0.1% of the total integrated luminosity.

After applying all the cluster vetoes, we require the events to contain at least one CSC or DT cluster with $N_{\text{hits}} > 50$. The minimum number of hits is chosen to exceed the number of hits that a muon is expected to create in either CSC or DT detectors. The presence of an MDS cluster passing the associated vetoes and identification criteria suppresses SM background by a factor exceeding 10^7 , whereas typical signal efficiencies are 25%–35%.

V. BACKGROUND ESTIMATION

After the event selections described in Sec. IV, two types of background events remain, in which the MDS cluster can be muon-induced or non-muon-induced. The non-muon-induced background involves a hard scattering process that produces a prompt lepton, and low momentum hadrons from pileup or an underlying event generate an MDS cluster. The dominant component of this background comes from W production, and subdominant contributions arise from QCD, $t\bar{t}$, or diboson production. The muon-induced background comes from $Z \rightarrow \mu\mu$ events, in which one of the two muons from the Z boson undergoes bremsstrahlung in the muon detector and produces an MDS cluster back to back with the other prompt muon, mimicking the configuration of a signal event. For the non-muon-induced background, which is present in both the prompt-muon and prompt-electron categories, we use an ‘‘ABCD’’ (matrix) method, which requires two variables that discriminate between signal and background and are independent of one another for the background. For the $Z \rightarrow \mu\mu$ background, which is present only in the

prompt-muon categories, the background estimation is derived from dedicated control regions in data.

In the ABCD method, we select the two independent variables to be (i) the azimuthal angle between the prompt lepton and the cluster centroid ($\Delta\phi_{\text{lep}}$) and (ii) N_{hits} . For non-muon-induced events, $\Delta\phi_{\text{lep}}$ is uniformly distributed and is independent of N_{hits} , because the cluster and lepton are produced from two independent processes. Figure 2 shows the shapes of the N_{hits} and $\Delta\phi_{\text{lep}}$ distribution for signal and background.

Two separate requirements, one on each variable, partition the two-dimensional space into four bins, A, B, C, and D, as illustrated in Fig. 3. The bin boundaries are optimized for the best expected search sensitivity, separately for each of the search categories. Since the HNL is primarily produced back to back with the prompt lepton, the bin with the best signal-to-background ratio is bin D defined as $\Delta\phi_{\text{lep}} > 2.8$ and $N_{\text{hits}} > 150$ or 200. Similarly, bin C is defined as $\Delta\phi_{\text{lep}} > 2.8$ and $N_{\text{hits}} \leq 150$ or 200, bin A is defined as $\Delta\phi_{\text{lep}} < 2.8$ and $N_{\text{hits}} > 150$ or 200, and bin B containing the least signal is defined as $\Delta\phi_{\text{lep}} < 2.8$ and $N_{\text{hits}} \leq 150$ or 200. The responses of the DT and CSC detectors to shower particles are generally different with CSC signal clusters having a larger hit multiplicity compared with DT signal clusters. The optimal bin boundary is found to be higher (200) for the CSC signal regions (SRs) compared with the DT SRs (150), with a similar signal efficiency of about 0.01% for an HNL with a $c\tau_0$ of 1 m. Because of the independence of the two variables, the expected background event rate in the signal-enriched bin D can be related to the other three bins by $\lambda_D = (\lambda_A\lambda_C)/\lambda_B$, where λ_X is the expected background event rate (i.e., the Poisson mean) in bin X. To account for a potential signal contribution to bins A, B, and C, a binned maximum likelihood fit is performed simultaneously in the four bins, with a common signal strength parameter scaling the signal yields in each bin. The background component of the fit is constrained to obey the ABCD relationship.

Because of the different background composition, we separate events with a selected prompt electron and a selected prompt muon into two disjoint categories. We also separate events with clusters in the CSC and DT detectors. Finally, for events in the category with a prompt muon and an MDS cluster in the DT detectors, we separate events into subcategories, which we call the DT-MB2 and DT-MB3/MB4, depending on whether the majority of the cluster’s hits fall in the MB2 station or the MB3 or MB4 station of the DT detector. This categorization is motivated by the fact that the background differs for clusters in the MB2 station because of the thinner shielding in front of it. The additional subcategories for DT clusters are advantageous for the prompt-muon channel because of its ability to suppress the additional $Z \rightarrow \mu\mu$ background as detailed below. This results in a total of five SRs.

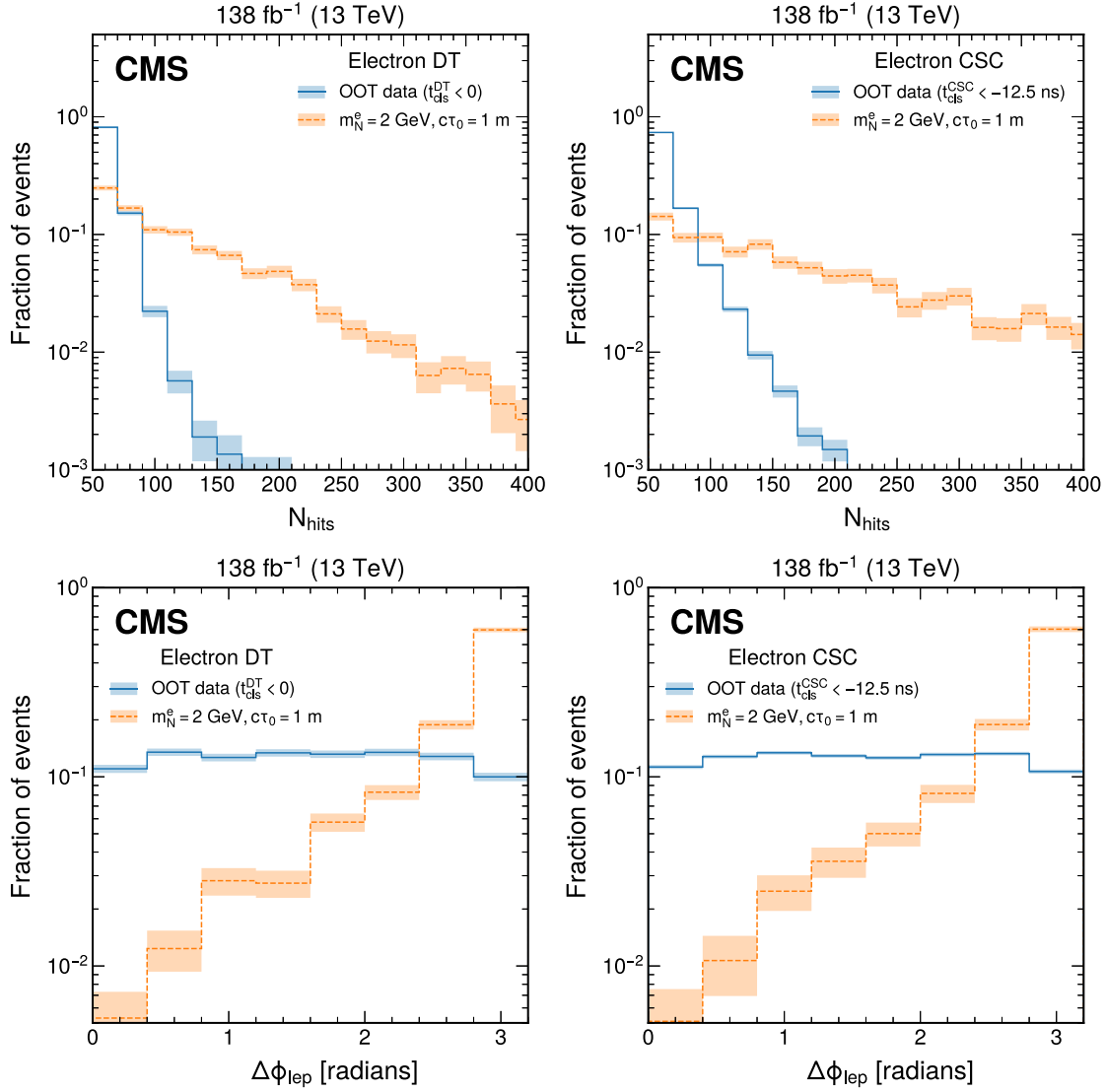


FIG. 2. Distribution of N_{hits} (upper) and $\Delta\phi_{\text{lep}}$ (lower) for DT clusters (left) and CSC clusters (right). Signal distributions of a Majorana HNL with $m_N = 2$ GeV and $c\tau_0 = 1$ m are compared with the OOT background distributions selected with $t_{\text{cluster}}^{\text{DT}}$ matched to bunch crossings earlier than the PV for DT clusters and $t_{\text{cluster}}^{\text{CSC}} < -12.5$ ns for CSC clusters. The centroids of the clusters in the signal events are required to be within $\Delta R = 0.4$ of the HNL's direction. The distributions are normalized to unit area. The shapes of the distributions shown are similar for the electron and muon channels.

The background estimation procedure is validated using events in the early OOT validation region (VR), defined as events passing all analysis selections except those related to the cluster time; instead, a negative cluster time is required. Additionally, the background estimation procedure is also checked for the in-time VR, defined as events with the azimuthal angle between the MDS cluster centroid position and the \vec{p}_T^{miss} : $\Delta\phi(\text{cluster}, \vec{p}_T^{\text{miss}}) > 0.7$. This VR is signal depleted because the MDS cluster and \vec{p}_T^{miss} tend to align, as described in Sec. IV A. The observed and predicted yields for these VRs are summarized in Table I and show that the ABCD method results are consistent with observed background yields. Similar consistencies are observed

when the validations are performed in both in-time and OOT VRs with looser N_{hits} requirements than in the SRs.

The ABCD background predictions for bin D of the SRs are listed in Table II for each of the event categories considered in this search. The event yields for the bins A, B, and C are shown, as well as the prediction for the background in the signal-enriched bin D.

In the prompt-muon event categories, $Z \rightarrow \mu\mu$ events constitute a significant background source that is not predicted by the ABCD method. The muon veto normally suppresses such backgrounds, but in rare cases, the muon may not be reconstructed in the muon system due to instrumental effects such as gaps between chambers.

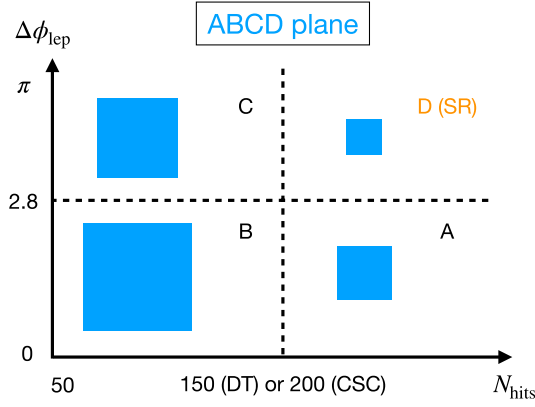


FIG. 3. Definition of the ABCD plane. The area of the blue squares illustrates the relative amount of expected events in each of the bins, with bins B and C having the majority of the event yields. Bin D is the signal region.

These nonreconstructed muons will lead to p_T^{miss} in the same direction as the cluster, and thus these events are not present in the VRs listed in Table I.

We define a $Z \rightarrow \mu\mu$ control region (CR) by inverting the MB1, or ME1/1 or ME1/2 hit veto requirements for MDS clusters in the DT or CSC detectors, respectively. After that, bin D will be dominated by the $Z \rightarrow \mu\mu$ background. The $Z \rightarrow \mu\mu$ expected background yield in bin D of the $Z \rightarrow \mu\mu$ CR is calculated as $\lambda_{Z \rightarrow \mu\mu, D}^{\text{CR}} = N_D^{\text{CR}} - \lambda_{\text{ABCD bkg}, D}^{\text{CR}}$, where N_D^{CR} is the observed data yield in bin D and $\lambda_{\text{ABCD bkg}, D}^{\text{CR}}$ is the ABCD method prediction. We extrapolate $\lambda_{Z \rightarrow \mu\mu, D}^{\text{CR}}$ to the SR by applying a transfer factor ζ , which estimates the pass-to-fail efficiency ratio for the MB1, ME1/1, and ME1/2 veto requirements for MDS clusters produced by muon bremsstrahlung.

The factor ζ is measured in a sample enhanced in MDS clusters produced by muon bremsstrahlung obtained by selecting dileptonic decays of tt pairs with an electron and muon in the final state. We select events with (i) one prompt electron matched to an electron trigger object; (ii) no

TABLE II. The event yields in the bins A, B, and C are shown in each of the event categories considered in the search, as well as the prefit prediction for the ABCD background in the signal-enriched bin D.

Channel	Region	A	B	C	D (prediction)
Muon	CSC	40	9316	1219	5.2 ± 0.8
Muon	DT-MB2	16	6512	1048	2.6 ± 0.7
Muon	DT-MB3/MB4	11	1011	229	2.5 ± 0.8
Electron	CSC	10	3993	497	1.2 ± 0.4
Electron	DT	15	3069	463	2.3 ± 0.6

reconstructed muon; (iii) one MDS cluster passing all the veto selections except the MB1, ME1/1, or ME1/2 vetoes; and (iv) exactly two additional jets with $p_T > 20$ GeV, $|\eta| < 2.4$ that pass the medium working point of the combined secondary vertex (CSV) b-tagging algorithm [80,81], which has an efficiency of 60% and a mistag rate of 1% for light-flavor or gluon jets. We also require that the MDS cluster is geometrically separated by $\Delta R > 0.8$ from the two jets that satisfy the CSV algorithm requirement to ensure that the MDS cluster is not produced by a punchthrough jet. These requirements result in an event sample that is pure in dileptonic tt events, in which both the electron and jets cannot produce the MDS cluster, thus ensuring that the MDS cluster is produced by the unreconstructed muon. We measure the ζ factors separately for MDS clusters in the DT and CSC detectors. We observed a linear dependence of ζ on N_{hits} in the MB2 category. To account for this dependence, we perform a linear fit to the data in the CR and evaluate the fitted function at $N_{\text{hits}} = 150$ as the ζ for the MB2 category. Finally, the expected $Z \rightarrow \mu\mu$ background contribution to bin D of the SR is calculated as $\lambda_{Z \rightarrow \mu\mu, D}^{\text{SR}} = \zeta \lambda_{Z \rightarrow \mu\mu, D}^{\text{CR}}$. Details of the $Z \rightarrow \mu\mu$ background prediction are summarized in Table III.

To validate the $Z \rightarrow \mu\mu$ background estimation method, we define another VR as a subset of the MB2 SR with

TABLE I. Validation of the ABCD method in the OOT and in-time validation regions. The predictions of the method for the signal bin (last column) are consistent with the observed number of events, shown in the second-to-last column.

Event category	Validation region	A	B	C	D	D (prediction)
Muon, DT-MB2	OOT	9	6924	944	0	1.2 ± 0.4
Muon, DT-MB3/MB4	OOT	11	593	86	1	1.6 ± 0.5
Muon, CSC	OOT	103	31074	4044	9	13.4 ± 1.3
Electron, DT	OOT	14	3301	366	2	1.6 ± 0.4
Electron, CSC	OOT	33	13774	1647	2	4.0 ± 0.7
Muon, DT-MB2	In time	10	5087	467	2	0.9 ± 0.3
Muon, DT-MB3/MB4	In time	9	785	107	2	1.2 ± 0.4
Muon, CSC	In time	31	7445	532	1	2.2 ± 0.4
Electron, DT	In time	8	2446	220	0	0.7 ± 0.3
Electron, CSC	In time	7	3217	227	0	0.5 ± 0.2

TABLE III. Summary of the $Z \rightarrow \mu\mu$ background estimate in different categories. The first three columns show the estimates in the $Z \rightarrow \mu\mu$ -enriched control region of the total background and its $Z \rightarrow \mu\mu$ and non-muon-induced components. The fourth column shows the transfer factors ζ used to predict the $Z \rightarrow \mu\mu$ background in the signal region, shown in the fifth column.

Region	N_D^{CR}	$\lambda_{\text{ABCD}}^{\text{CR}}$	$\lambda_{\text{bkg,D}}^{\text{CR}}$	$\lambda_{Z \rightarrow \mu\mu, D}^{\text{CR}}$	ζ (%)	$\lambda_{Z \rightarrow \mu\mu, D}^{\text{SR}}$
CSC	129	45 ± 2	84 ± 12	(4.8 ± 1.3)	3.9 ± 1.2	
DT-MB2	35	12.2 ± 1.5	22.8 ± 6.1	(36 ± 31)	8.2 ± 7.4	
DT-MB3/MB4	6	2.9 ± 0.7	3.1 ± 2.6	(2 ± 1)	0.06 ± 0.06	

$N_{\text{hits}} \leq 120$ which is expected to have a negligible signal contribution. In this VR, we define the bin boundaries for the ABCD method to be at 2.8 in $\Delta\phi_{\text{lep}}$ and at 110 in N_{hits} . We perform the prediction of the $Z \rightarrow \mu\mu$ and non-muon-induced background events using the same method applied to the full SR and obtain predictions of 2.7 ± 1.6 for the $Z \rightarrow \mu\mu$ background and 9.9 ± 1.3 for the other background, for a total background prediction of 12.6 ± 2.1 events. We observe an event yield of 12, which is consistent with our background predictions.

VI. SYSTEMATIC UNCERTAINTIES

The dominant systematic uncertainties in this search are those in the background predictions. The main source of uncertainty for the ABCD method arises from the statistical

uncertainties of the background-enriched bins A, B, and C. This uncertainty accounts for 27% and 22% (40% and 18%) of the size of the total background in the electron and muon categories, respectively, for MDS clusters in the DT (CSC) detector.

For the prompt-muon categories, an uncertainty in the estimate of the $Z \rightarrow \mu\mu$ background also contributes significantly to the total uncertainty. The uncertainty for that background prediction arises from the statistical uncertainty of the ζ measurement, accounting for about 72%, 2%, and 15% of the size of the total background in the muon channel for DT-MB2, DT-MB3/MB4, and CSC clusters, respectively.

Systematic uncertainties in the signal yield include both theoretical and instrumentation effects. The theoretical uncertainty in the inclusive cross section of W boson production is 3.8%, which is dominated by the parton distribution function uncertainty. The uncertainty in the W boson p_T distribution is estimated by varying the renormalization and factorization scales by a factor of 2, separately and coherently, and evaluating the size of the envelope in the resulting signal yield, which is found to be 1.6%. The uncertainty of parton shower modeling is estimated similarly by varying the renormalization scales for parton showers and is found to be 4%.

The accuracy of the CMS simulation and the Geant4 software in describing the details of the evolution of electromagnetic and hadronic showers has already been validated extensively in past measurements. However, the

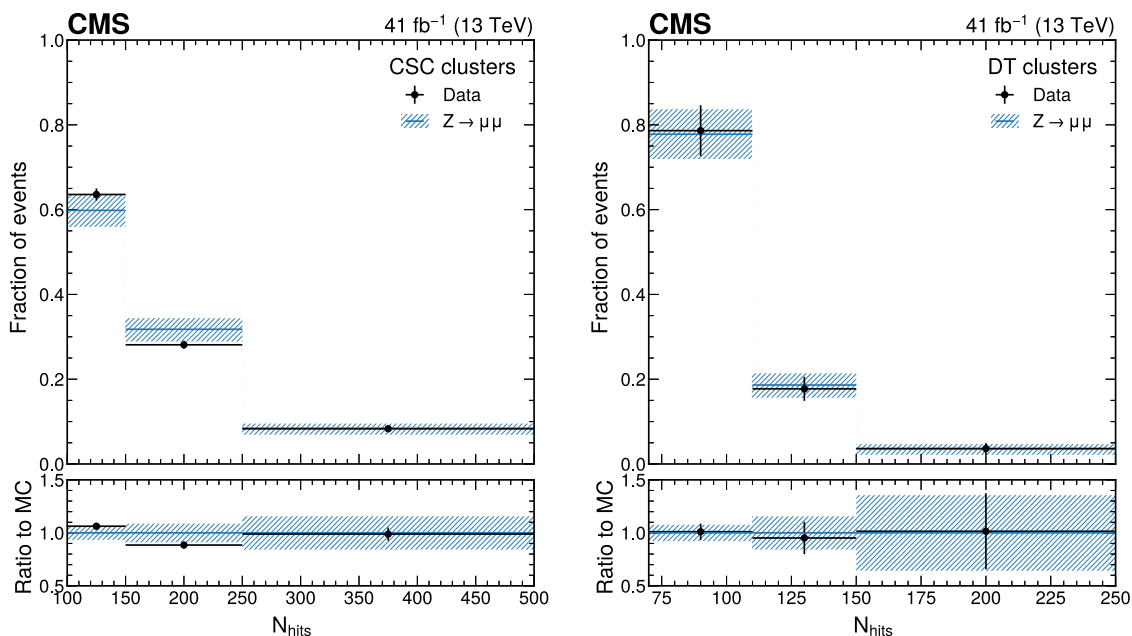


FIG. 4. Comparison of N_{hits} distributions for events with muons from $Z \rightarrow \mu\mu$ between data and simulation, for CSC clusters (left) and DT clusters (right), using data collected in 2017 and the simulation of the corresponding data-taking conditions. The data sample is selected by requiring a two-muon-invariant mass consistent with a Z boson and one of the muons is matched to an MDS cluster. Data-to-simulation correction factors are applied to the $Z \rightarrow \mu\mu$ simulation. Only statistical uncertainties are included in the figure. Distributions made using data collected in 2016 and 2018 are found to have similar shape as the 2017 data sample.

accuracy of the CMS simulation implementation of the response of the muon detectors in an environment with a large multiplicity of secondary particles, which affects the simulated reconstruction efficiencies in the SR, has not been explicitly verified. This aspect is validated by comparing clusters produced in $Z \rightarrow \mu\mu$ data and simulated events, in which one of the muons undergoes bremsstrahlung in the muon detectors and the associated photon produces an electromagnetic shower. With this comparison, we derive the uncertainties in the cluster reconstruction efficiency for both CSC and DT clusters in simulation; they account for 16% and 13% of the signal yield for the DT and CSC categories, respectively. These uncertainties apply to both electromagnetic and hadronic showers. Figure 4 illustrates this validation of the cluster simulation. Data-to-simulation corrections on other cluster properties are also derived with the same method, and the uncertainties in the corrections are propagated as systematic uncertainties. For DT clusters, a correction of 6.8% is applied for the MB1 veto efficiency, with an uncertainty of 7.4%. For CSC clusters, corrections are applied to account for the hit and segment vetoes (2.8%), muon veto (6.8%), and jet veto efficiencies (2.1%), with uncertainties of 0.1%, 4.5%, and 0.06%, respectively. Additionally, the uncertainties on efficiencies of the CSC cluster identification, time, and time spread requirements are estimated to be 5%, 0.9%, and 2.8%, respectively. In data, only the reconstructed hits that

have at least two cathode hits in different CSC layers and match a given predefined pattern are read out. In contrast, this readout condition is assumed to be satisfied in the signal simulation, which could lead to an overestimation of the N_{hits} in signal clusters. We estimated this effect by excluding those chambers with less than 6 hits in signal clusters and assigning the change in signal efficiency (1%) as an uncertainty.

We also propagate additional systematic uncertainties that have a minor impact on the signal yield prediction. They include uncertainties due to pileup, integrated luminosity, jet energy scale, and prompt electron or muon trigger and selection efficiencies. The integrated luminosities for the 2016, 2017, and 2018 data-taking years have 1.2%–2.5% individual uncertainties [62–64], while the overall uncertainty for the 2016–2018 period is 1.6%.

Finally, the uncertainties on the signal yields from the limited numbers of simulated events are in the ranges 5%–10% depending on m_N and lifetime. Theoretical and experimental uncertainties that are not related to the clusters are treated as fully correlated across different event categories. Experimental uncertainties related to the clusters are treated as fully uncorrelated. A full list of systematic uncertainties affecting the predicted signal yield is shown in Table IV.

VII. RESULTS AND INTERPRETATION

Figure 5 shows the expected and observed number of events in the SRs of the different event categories and the corresponding background predictions. The observed yields agree with the predicted background in all channels.

No excess of data events over the background prediction is observed, and upper limits on the HNL production cross sections are evaluated using the CL_s criterion [82,83], with the binned profile likelihood ratio [84] as the test statistic. The likelihood is constructed as the product of Poisson

TABLE IV. Summary of systematic uncertainties affecting the signal yield prediction. For DT clusters, the systematic uncertainties due to jet and muon vetoes are found to be negligible and are omitted. The uncertainties are reported relative to their impact on the predicted signal yield.

Systematic uncertainty	Object	Size of uncertainty (%)
Integrated luminosity	...	1.6
Pileup	...	1
W boson cross section	...	3.8
W boson p_T	...	1.6
Parton shower modeling	...	4
Trigger	Muon	<0.1
Identification	Muon	0.4–0.5
Isolation	Muon	0.2–0.6
Trigger	Electron	0.2–0.3
Identification	Electron	2.2–8.0
Jet energy scale	p_T^{miss}	2.0
Cluster reconstruction	CSC cluster	13
Cutoff-based ID	CSC cluster	5.1
Jet veto	CSC cluster	0.06
Muon veto	CSC cluster	4.5
CSC readout	CSC cluster	1.0
Hits and segment veto	CSC cluster	0.1
Cluster time	CSC cluster	0.9
Cluster time spread	CSC cluster	2.8
Cluster reconstruction	DT cluster	16
MB1 veto	DT cluster	7.4

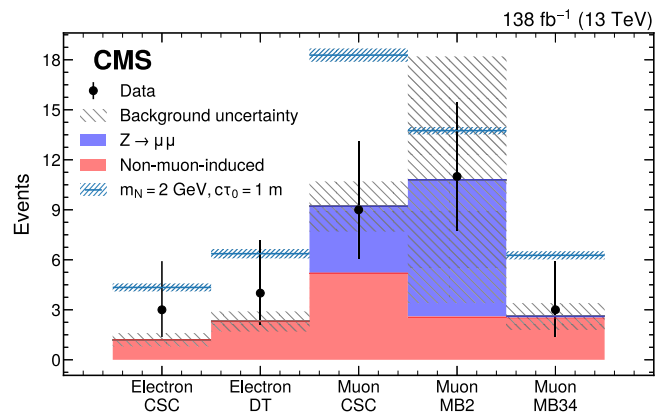


FIG. 5. The expected and observed number of events in the signal region (bin D) of different event categories. Signal yields of a 2 GeV Majorana HNL with the mean proper decay length of 1 m are added to the expected background.

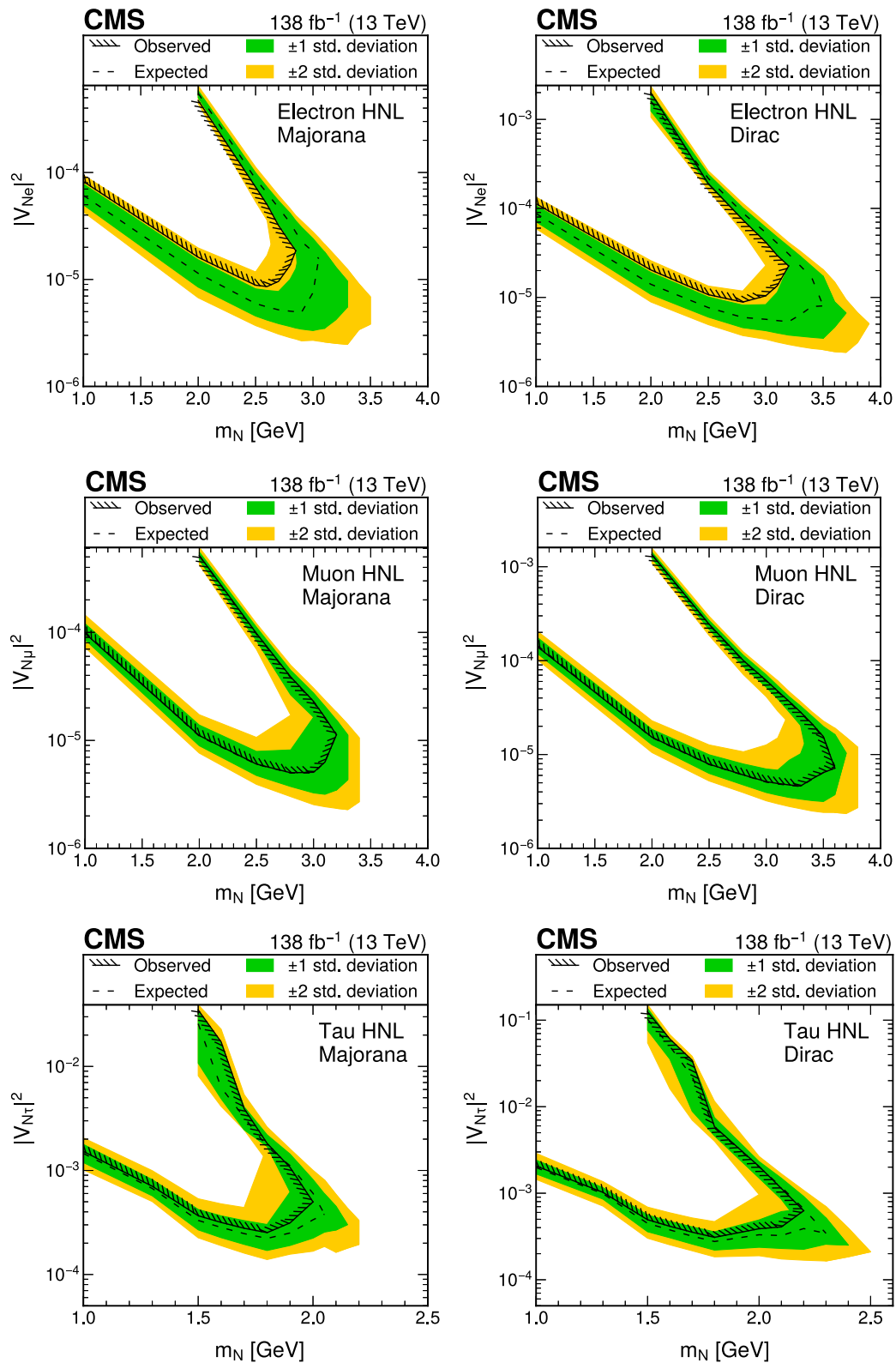


FIG. 6. Expected and observed upper 95% CL limits on $|V_{Ne}|^2$ (upper), $|V_{N\mu}|^2$ (middle), and $|V_{N\tau}|^2$ (lower) as functions of the HNL mass (m_N) for a Majorana (left) and Dirac (right) type HNL. The τ neutrino mixing limit is obtained by combining the results from the electron and muon channels. For these limit calculations, the HNL is assumed to mix with a single lepton flavor state only. The differences between the expected and observed limits on $|V_{N\mu}|^2$ are not visible in this figure.

TABLE V. Excluded ranges of $|V_{N\ell}|^2$ for Majorana and Dirac type HNLs at select HNL masses. The chosen HNL masses are those at which the excluded values of $|V_{N\ell}|^2$ have the smallest magnitude.

Mixing parameter	HNL type	m_N (GeV)	Excluded range at 95% CL
$ V_{Ne} ^2$	Majorana	2.6	8.6×10^{-6} – 5.0×10^{-5}
$ V_{N\mu} ^2$	Majorana	2.8	5.0×10^{-6} – 3.9×10^{-5}
$ V_{N\tau} ^2$	Majorana	1.8	2.5×10^{-4} – 1.8×10^{-3}
$ V_{Ne} ^2$	Dirac	2.8	8.9×10^{-6} – 7.5×10^{-5}
$ V_{N\mu} ^2$	Dirac	3.3	4.6×10^{-6} – 2.8×10^{-5}
$ V_{N\tau} ^2$	Dirac	1.8	3.1×10^{-4} – 5.9×10^{-3}

distributions with mean values based on the predicted event rates across all five event categories. The predicted event rates in each bin include the background yields predicted with the ABCD method plus the $Z \rightarrow \mu\mu$ background

contribution for bin D and the signal yields obtained from simulated events. Systematic uncertainties in the predicted event rates are incorporated in the likelihood as nuisance parameters with log-normal constraints. The asymptotic formulas [85] are used to evaluate the exclusion limits for each HNL signal scenario. The exclusion limits derived from the asymptotic formulas are consistent within 10% with those based on pseudoexperiments.

Due to the lower p_T thresholds for the prompt muons, the signal yields in the muon channel are larger than those of the electron channels for the same m_N and lifetime. However, the presence of the $Z \rightarrow \mu\mu$ background reduces the overall sensitivity of the muon channel to a level comparable to the electron channel. For both the muon and electron channels, the CSC category contributes the majority of the overall sensitivity. This is because the CSC category has smaller background rates compared with the DT category, hence retaining more signal events at the optimal thresholds for background rejection.

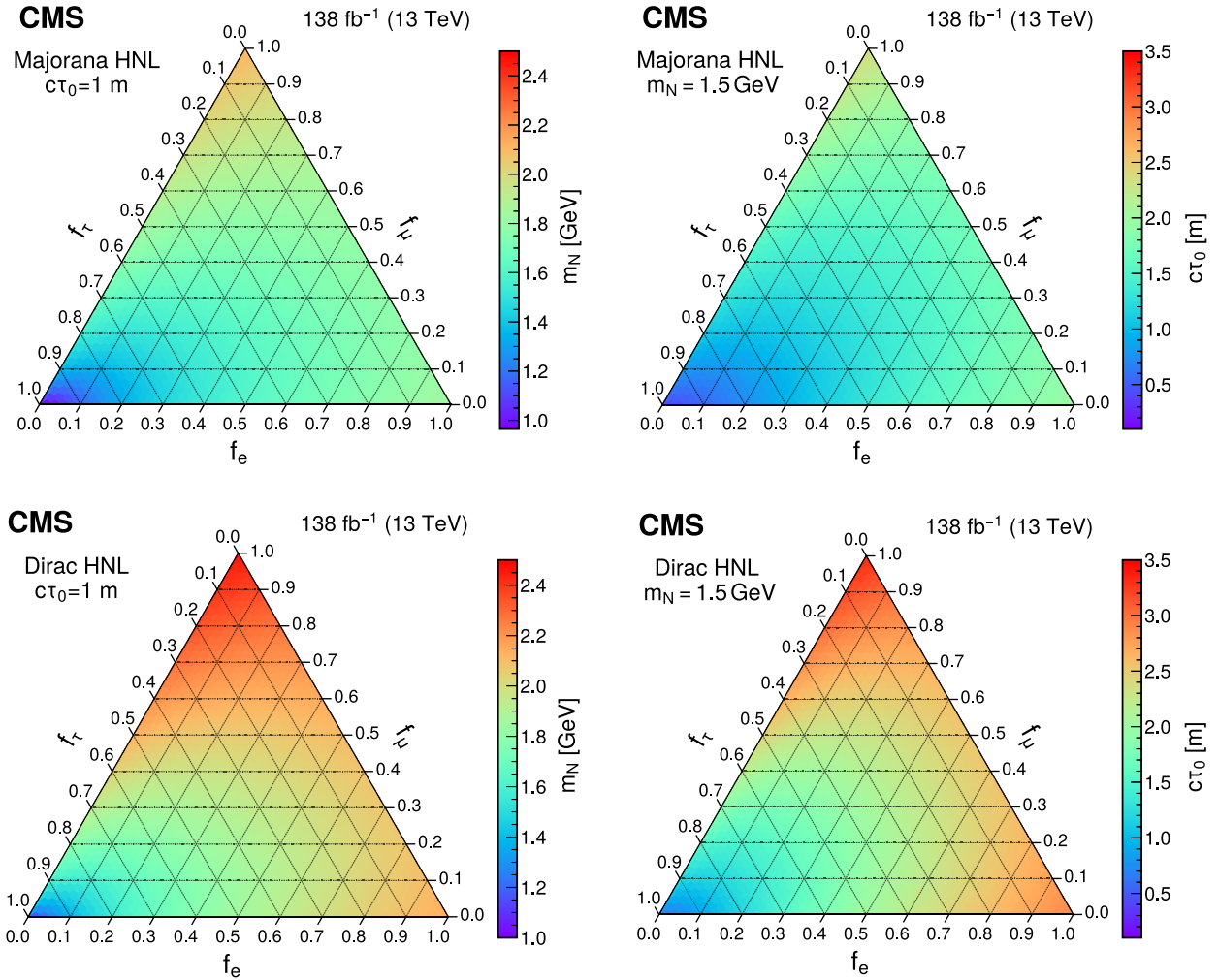


FIG. 7. The largest values of the Majorana (upper) and Dirac (lower) HNL mass (left) and mean proper decay length (right) parameters that are excluded at 95% CL are shown as a function of the mixing matrix elements squared ratios f_ℓ with the three lepton generations, considering a mean proper decay length of 1 m and a fixed mass of 1.5 GeV, respectively.

Figure 6 shows the expected and observed upper limits at 95% confidence level (CL) on the HNL mixing parameters $|V_{Ne}|^2$, $|V_{N\mu}|^2$, and $|V_{N\tau}|^2$, as functions of m_N for the Majorana and Dirac HNL interpretations. For $|V_{Ne}|^2$ ($|V_{N\mu}|^2$), only events passing the electron (muon) selections are used to evaluate the limits. For $|V_{N\tau}|^2$, both the events passing the electron and muon selections are used, because the prompt τ lepton can decay into an electron or muon. The limits of $|V_{N\ell}|^2$ versus m_N feature an upper branch (short lifetime) and a lower branch (long lifetime). The lower acceptance in the short lifetime branch is compensated by an increased cross section and thus achieves a signal yield comparable with the long lifetime branch. Below m_N of 2.0 (1.5) GeV for electron or muon (τ) type HNLs, we do not calculate a limit in the short lifetime branch because the signal acceptance in the muon system approaches zero and renders the calculation inaccurate. Furthermore, in that region other experimental results [27,28,30] place more stringent limits. Table V summarizes the observed limits on $|V_{N\ell}|^2$ for Majorana and Dirac type HNL of this search. This result sets the most stringent limits to date in $|V_{N\ell}|^2$ for HNL masses in the range 2.1–3.0 (1.9–3.3) GeV for electron (muon) neutrino mixing parameters [43]. Above 3.0 (3.3) GeV, previous CMS results [38] place tighter limits on electron (muon) mixing parameters.

Signal yields for mixing among several different lepton flavors are obtained by reweighting the single flavor signal yields with the same m_N and $c\tau_0$. In this case, the signal yields for multiple neutrino species mixing are proportional to $|V_{N\ell}|^2$. The ratio of $|V_{N\ell}|^2$ to the sum of the mixing matrix elements squared is defined as $f_\ell = |V_{N\ell}|^2 / (|V_{Ne}|^2 + |V_{N\mu}|^2 + |V_{N\tau}|^2)$ and sums to unity by construction. For a fixed value of m_N ($c\tau_0$), we scan the three f_ℓ parameters and exclude a range in the $c\tau_0$ (m_N) parameter for each set of f_ℓ values. On the left (right) of Fig. 7, we show the largest values of m_N ($c\tau_0$) that are excluded as a function of the f_ℓ parameters. The sensitivity across the f_ℓ plane varies mainly because of the different trigger and reconstruction efficiencies of the prompt lepton. The limits at $f_e : f_\mu : f_\tau = 0 : \frac{1}{2} : \frac{1}{2}$ and $\frac{1}{3} : \frac{1}{3} : \frac{1}{3}$ probe parameter space consistent with the constraints from neutrino oscillation data in the minimal seesaw scenarios [86].

VIII. SUMMARY

A search for long-lived Dirac or Majorana HNLs has been performed using proton-proton collision data at $\sqrt{s} = 13$ TeV, corresponding to an integrated luminosity of 138 fb^{-1} . The search targets events with one prompt electron or muon and an MDS that would result from HNL decays occurring in the CMS muon detector. The presence of the MDS signature along with the associated vetoes and identification criteria suppresses the standard model background by a factor exceeding 10^7 , while maintaining typical signal efficiencies of 25%–35%. No significant

excess over the standard model background is observed. The results are interpreted as 95% confidence level limits on the HNL mixing matrix elements squared $|V_{Ne}|^2$, $|V_{N\mu}|^2$, and $|V_{N\tau}|^2$. We also present limits on the HNL mass and mean proper decay length as a function of the mixing matrix element squared fractions to the three lepton generations. The most stringent limits to date for HNLs in the mass range of 2.1–3.0 (1.9–3.3) GeV are set, reaching squared mixing matrix element values as low as $8.6(4.6) \times 10^{-6}$ in the electron (muon) channel.

ACKNOWLEDGMENTS

We congratulate our colleagues in the CERN accelerator departments for the excellent performance of the LHC and thank the technical and administrative staffs at CERN and at other CMS institutes for their contributions to the success of the CMS effort. In addition, we gratefully acknowledge the computing centers and personnel of the Worldwide LHC Computing Grid and other centers for delivering so effectively the computing infrastructure essential to our analyses. Finally, we acknowledge the enduring support for the construction and operation of the LHC, the CMS detector, and the supporting computing infrastructure provided by the following funding agencies: SC (Armenia); BMBWF and FWF (Austria); FNRS and FWO (Belgium); CNPq, CAPES, FAPERJ, FAPERGS, and FAPESP (Brazil); MES and BNSF (Bulgaria); CERN; CAS, MoST, and NSFC (China); Minciencias (Colombia); MSES and CSF (Croatia); RIF (Cyprus); SENESCYT (Ecuador); ERC PRG, RVTT3, and MoER TK202 (Estonia); Academy of Finland, MEC, and HIP (Finland); CEA and CNRS/IN2P3 (France); SRNSF (Georgia); BMBF, DFG, and HGF (Germany); GSRI (Greece); NKFIH (Hungary); DAE and DST (India); IPM (Iran); SFI (Ireland); INFN (Italy); MSIP and NRF (Republic of Korea); MES (Latvia); LMTLT (Lithuania); MOE and UM (Malaysia); BUAP, CINVESTAV, CONACYT, LNS, SEP, and UASLP-FAI (Mexico); MOS (Montenegro); MBIE (New Zealand); PAEC (Pakistan); MES and NSC (Poland); FCT (Portugal); MESTD (Serbia); MCIN/AEI and PCTI (Spain); MOSTR (Sri Lanka); Swiss Funding Agencies (Switzerland); MST (Taipei); MHESI and NSTDA (Thailand); TUBITAK and TENMAK (Turkey); NASU (Ukraine); STFC (United Kingdom); DOE and NSF (U.S.). Individuals have received support from the Marie-Curie program and the European Research Council and Horizon 2020 Grant, Contracts No. 675440, No. 724704, No. 752730, No. 758316, No. 765710, No. 824093, No. 101115353, and COST Action CA16108 (European Union); the Leventis Foundation; the Alfred P. Sloan Foundation; the Alexander von Humboldt Foundation; the Science Committee, Project No. 22r1-037 (Armenia); the Belgian Federal Science Policy Office; the Fonds pour la Formation à la Recherche dans l'Industrie et dans

l’Agriculture (FRIA-Belgium); the Agentschap voor Innovatie door Wetenschap en Technologie (IWT-Belgium); the F.R.S.-FNRS and FWO (Belgium) under the “Excellence of Science—EOS”—be.h Project No. 30820817; the Beijing Municipal Science and Technology Commission, No. Z191100007219010 and Fundamental Research Funds for the Central Universities (China); the Ministry of Education, Youth and Sports (MEYS) of the Czech Republic; the Shota Rustaveli National Science Foundation, Grant No. FR-22-985 (Georgia); the Deutsche Forschungsgemeinschaft (DFG), under Germany’s Excellence Strategy—EXC 2121 “Quantum Universe”—390833306 and under Project No. 400140256—GRK2497; the Hellenic Foundation for Research and Innovation (HFRI), Project No. 2288 (Greece); the Hungarian Academy of Sciences, the New National Excellence Program—ÚNKP, the NKFIH Research Grants No. K 124845, No. K 124850, No. K 128713, No. K 128786, No. K 129058, No. K 131991, No. K 133046, No. K 138136, No. K 143460, No. K 143477, No. 2020-2.2.1-ED-2021-00181, and No. TKP2021-NKTA-64 (Hungary); the Council of Science and Industrial Research, India; ICSC—National Research Center for High Performance Computing,

Big Data and Quantum Computing, funded by the NextGenerationEU program (Italy); the Latvian Council of Science; the Ministry of Education and Science, Project No. 2022/WK/14, and the National Science Center, Contracts Opus No. 2021/41/B/ST2/01369 and No. 2021/43/B/ST2/01552 (Poland); the Fundação para a Ciência e a Tecnologia, Grant No. CEECIND/01334/2018 (Portugal); the National Priorities Research Program by Qatar National Research Fund; MCIN/AEI/10.13039/501100011033, ERDF “A way of making Europe,” and the Programa Estatal de Fomento de la Investigación Científica y Técnica de Excelencia María de Maeztu, Grant No. MDM-2017-0765, and Programa Severo Ochoa del Principado de Asturias (Spain); the Chulalongkorn Academic into Its Second Century Project Advancement Project, and the National Science, Research and Innovation Fund via the Program Management Unit for Human Resources and Institutional Development, Research and Innovation, Grant No. B37G660013 (Thailand); the Kavli Foundation; the Nvidia Corporation; the SuperMicro Corporation; the Welch Foundation, Contract No. C-1845; and the Weston Havens Foundation (USA).

-
- [1] Y. Fukuda *et al.* (Super-Kamiokande Collaboration), Evidence for oscillation of atmospheric neutrinos, *Phys. Rev. Lett.* **81**, 1562 (1998).
- [2] Q. Ahmad *et al.* (SNO Collaboration), Direct evidence for neutrino flavor transformation from neutral-current interactions in the Sudbury Neutrino Observatory, *Phys. Rev. Lett.* **89**, 011301 (2002).
- [3] K. Eguchi *et al.* (KamLAND Collaboration), First results from KamLAND: Evidence for reactor antineutrino disappearance, *Phys. Rev. Lett.* **90**, 021802 (2003).
- [4] S. Bilenyk, Neutrino oscillations: From a historical perspective to the present status, *Nucl. Phys.* **B908**, 2 (2016).
- [5] S. Roy Choudhury and S. Hannestad, Updated results on neutrino mass and mass hierarchy from cosmology with Planck 2018 likelihoods, *J. Cosmol. Astropart. Phys.* **07** (2020) 037.
- [6] M. Ivanov, M. Simonović, and M. Zaldarriaga, Cosmological parameters and neutrino masses from the final Planck and full-shape BOSS data, *Phys. Rev. D* **101**, 083504 (2020).
- [7] J. Formaggio, A. de Gouvêa, and R. Robertson, Direct measurements of neutrino mass, *Phys. Rep.* **914**, 1 (2021).
- [8] P. Minkowski, $\mu \rightarrow e\gamma$ at a rate of one out of 10^9 muon decays?, *Phys. Lett.* **67B**, 421 (1977).
- [9] T. Yanagida, Horizontal symmetry and masses of neutrinos, *Prog. Theor. Phys.* **64**, 1103 (1980).
- [10] M. Gell-Mann, P. Ramond, and R. Slansky, Complex spinors and unified theories, in *Supergravity*, edited by P. van Nieuwenhuizen and D.Z. Freedman (North Holland Publishing, 1979), p. 315.
- [11] S. Glashow, The future of elementary particle physics, *NATO Sci. Ser. B* **61**, 687 (1980).
- [12] R.N. Mohapatra and G. Senjanović, Neutrino mass and spontaneous parity nonconservation, *Phys. Rev. Lett.* **44**, 912 (1980).
- [13] J. Schechter and J. W. F. Valle, Neutrino masses in $SU(2) \otimes U(1)$ theories, *Phys. Rev. D* **22**, 2227 (1980).
- [14] R. E. Shrock, General theory of weak leptonic and semi-leptonic decays. I. Leptonic pseudoscalar meson decays, with associated tests for, and bounds on, neutrino masses and lepton mixing, *Phys. Rev. D* **24**, 1232 (1981).
- [15] Y. Cai, T. Han, T. Li, and R. Ruiz, Lepton number violation: Seesaw models and their collider tests, *Front. Phys.* **6**, 40 (2018).
- [16] Z. Maki, M. Nakagawa, and S. Sakata, Remarks on the unified model of elementary particles, *Prog. Theor. Phys.* **28**, 870 (1962).
- [17] B. Pontecorvo, Neutrino experiments and the problem of conservation of leptonic charge, *Zh. Eksp. Teor. Fiz.* **53**, 1717 (1967).
- [18] A. Das, P. Konar, and S. Majhi, Production of heavy neutrino in next-to-leading order QCD at the LHC and beyond, *J. High Energy Phys.* **06** (2016) 019.
- [19] A. Das and N. Okada, Bounds on heavy Majorana neutrinos in type-I seesaw and implications for collider searches, *Phys. Lett. B* **774**, 32 (2017).
- [20] G. Cottin, J. C. Helo, M. Hirsch, C. Peña, C. Wang, and S. Xie, Long-lived heavy neutral leptons with a displaced shower signature at CMS, *J. High Energy Phys.* **02** (2023) 011.

- [21] K. Bondarenko, A. Boyarsky, D. Gorbunov, and O. Ruchayskiy, Phenomenology of GeV-scale heavy neutral leptons, *J. High Energy Phys.* **11** (2018) 032.
- [22] M. Fukugita and T. Yanagida, Baryogenesis without grand unification, *Phys. Lett. B* **174**, 45 (1986).
- [23] E. Chun, G. Cvetič, P. Dev, M. Drewes, C. Fong, B. Garbrecht, T. Hambye, J. Harz, J. Hernández, C. Kim, E. Molinaro, E. Nardi, J. Racker, N. Rius, and J. Zamora-Saa, Probing leptogenesis, *Int. J. Mod. Phys. A* **33**, 1842005 (2018).
- [24] A. Boyarsky, M. Drewes, T. Lasserre, S. Mertens, and O. Ruchayskiy, Sterile neutrino dark matter, *Prog. Part. Nucl. Phys.* **104**, 1 (2019).
- [25] V. Cirigliano, W. Dekens, J. de Vries, K. Fuyuto, E. Mereghetti, and R. Ruiz, Leptonic anomalous magnetic moments in ν SMEFT, *J. High Energy Phys.* **08** (2021) 103.
- [26] D. P. Aguillard *et al.* (Muon $g-2$ Collaboration), Measurement of the positive muon anomalous magnetic moment to 0.20 ppm, *Phys. Rev. Lett.* **131**, 161802 (2023).
- [27] A. M. Cooper-Sarkar *et al.* (WA66 Collaboration), Search for heavy neutrino decays in the BEBC beam dump experiment, *Phys. Lett.* **160B**, 207 (1985).
- [28] F. Bergsma *et al.* (CHARM Collaboration), A search for decays of heavy neutrinos in the mass range 0.5–2.8 GeV, *Phys. Lett.* **166B**, 473 (1986).
- [29] DELPHI Collaboration, Search for neutral heavy leptons produced in Z decays, *Z. Phys. C* **74**, 57 (1997); **75**, 580(E) (1997).
- [30] A. Vaitaitis *et al.* (NuTeV(E815) Collaboration), Search for neutral heavy leptons in a high-energy neutrino beam, *Phys. Rev. Lett.* **83**, 4943 (1999).
- [31] D. Liventsev *et al.* (Belle Collaboration), Search for heavy neutrinos at Belle, *Phys. Rev. D* **87**, 071102 (2013); **95**, 099903(E) (2017).
- [32] F. F. Deppisch, P. S. Bhupal Dev, and A. Pilaftsis, Neutrinos and collider physics, *New J. Phys.* **17**, 075019 (2015).
- [33] J. Beacham *et al.*, Physics beyond colliders at CERN: Beyond the standard model working group report, *J. Phys. G* **47**, 010501 (2020).
- [34] ATLAS Collaboration, Search for heavy neutral leptons in decays of W bosons produced in 13 TeV pp collisions using prompt and displaced signatures with the ATLAS detector, *J. High Energy Phys.* **10** (2019) 265.
- [35] ATLAS Collaboration, Search for heavy neutral leptons in decays of W bosons using a dilepton displaced vertex in $\sqrt{s} = 13$ TeV pp collisions with the ATLAS detector, *Phys. Rev. Lett.* **131**, 061803 (2023).
- [36] CMS Collaboration, Search for heavy neutral leptons in events with three charged leptons in proton-proton collisions at $\sqrt{s} = 13$ TeV, *Phys. Rev. Lett.* **120**, 221801 (2018).
- [37] CMS Collaboration, Search for heavy Majorana neutrinos in same-sign dilepton channels in proton-proton collisions at $\sqrt{s} = 13$ TeV, *J. High Energy Phys.* **01** (2019) 122.
- [38] CMS Collaboration, Search for long-lived heavy neutral leptons with displaced vertices in proton-proton collisions at $\sqrt{s} = 13$ TeV, *J. High Energy Phys.* **07** (2022) 081.
- [39] LHCb Collaboration, Search for heavy neutral leptons in $W^+ \rightarrow \mu^+ \mu^\pm \text{jet}$ decays, *Eur. Phys. J. C* **81**, 248 (2021).
- [40] LHCb Collaboration, Search for long-lived particles decaying to $e^\pm \mu^\mp \nu$, *Eur. Phys. J. C* **81**, 261 (2021).
- [41] CMS Collaboration, Search for long-lived heavy neutral leptons with lepton flavour conserving or violating decays to a jet and a charged lepton, *J. High Energy Phys.* **03** (2024) 105.
- [42] CMS Collaboration, Search for long-lived particles decaying in the CMS end cap muon detectors in proton-proton collisions at $\sqrt{s} = 13$ TeV, *Phys. Rev. Lett.* **127**, 261804 (2021).
- [43] The CMS collaboration, Search for long-lived heavy neutral leptons decaying in the CMS muon detectors in proton-proton collisions at $\sqrt{s} = 13$ TeV (2023), [10.17182/hepdata.146757](https://arxiv.org/abs/10.17182/hepdata.146757).
- [44] CMS Collaboration, Performance of the CMS drift tube chambers with cosmic rays, *J. Instrum.* **5**, T03015 (2010).
- [45] CMS Collaboration, Performance of the CMS level-1 trigger in proton-proton collisions at $\sqrt{s} = 13$ TeV, *J. Instrum.* **15**, P10017 (2020).
- [46] CMS Collaboration, The CMS trigger system, *J. Instrum.* **12**, P01020 (2017).
- [47] CMS Collaboration, The CMS experiment at the CERN LHC, *J. Instrum.* **3**, S08004 (2008).
- [48] P. Nason, A new method for combining NLO QCD with shower Monte Carlo algorithms, *J. High Energy Phys.* **11** (2004) 040.
- [49] S. Frixione, P. Nason, and C. Oleari, Matching NLO QCD computations with parton shower simulations: The POWHEG method, *J. High Energy Phys.* **11** (2007) 070.
- [50] S. Alioli, P. Nason, C. Oleari, and E. Re, A general framework for implementing NLO calculations in shower Monte Carlo programs: The POWHEG box, *J. High Energy Phys.* **06** (2010) 043.
- [51] R. Gavin, Y. Li, F. Petriello, and S. Quackenbush, FEWZ 2.0: A code for hadronic Z production at next-to-next-to-leading order, *Comput. Phys. Commun.* **182**, 2388 (2011).
- [52] R. Gavin, Y. Li, F. Petriello, and S. Quackenbush, W physics at the LHC with FEWZ 2.1, *Comput. Phys. Commun.* **184**, 208 (2013).
- [53] J. Alwall, R. Frederix, S. Frixione, V. Hirschi, F. Maltoni, O. Mattelaer, H. S. Shao, T. Stelzer, P. Torrielli, and M. Zaro, The automated computation of tree-level and next-to-leading order differential cross sections, and their matching to parton shower simulations, *J. High Energy Phys.* **07** (2014) 079.
- [54] D. Alva, T. Han, and R. Ruiz, Heavy Majorana neutrinos from $W\gamma$ fusion at hadron colliders, *J. High Energy Phys.* **02** (2015) 072.
- [55] C. Degrande, O. Mattelaer, R. Ruiz, and J. Turner, Fully-automated precision predictions for heavy neutrino production mechanisms at hadron colliders, *Phys. Rev. D* **94**, 053002 (2016).
- [56] S. Pascoli, R. Ruiz, and C. Weiland, Heavy neutrinos with dynamic jet vetoes: Multilepton searches at $\sqrt{s} = 14, 27$, and 100 TeV, *J. High Energy Phys.* **06** (2019) 049.
- [57] T. Sjöstrand, S. Ask, J. R. Christiansen, R. Corke, N. Desai, P. Ilten, S. Mrenna, S. Prestel, C. O. Rasmussen, and P. Z. Skands, An introduction to PYTHIA 8.2, *Comput. Phys. Commun.* **191**, 159 (2015).
- [58] Y. Li and F. Petriello, Combining QCD and electroweak corrections to dilepton production in FEWZ, *Phys. Rev. D* **86**, 094034 (2012).

- [59] S. Camarda, M. Boonekamp, G. Bozzi, S. Catani, L. Cieri, J. Cuth, G. Ferrera, D. de Florian, A. Glazov, M. Grazzini, M. G. Vincter, and M. Schott, *DYTurbo*: Fast predictions for Drell-Yan processes, *Eur. Phys. J. C* **80**, 251 (2020).
- [60] S. Camarda, L. Cieri, and G. Ferrera, Drell-Yan lepton-pair production: q_T resummation at N^3 LL accuracy and fiducial cross sections at N^3 LO, *Phys. Rev. D* **104**, L111503 (2021).
- [61] S. Agostinelli *et al.* (GEANT4 Collaboration), *Geant4*—A simulation toolkit, *Nucl. Instrum. Methods Phys. Res., Sect. A* **506**, 250 (2003).
- [62] CMS Collaboration, Precision luminosity measurement in proton-proton collisions at $\sqrt{s} = 13$ TeV in 2015 and 2016 at CMS, *Eur. Phys. J. C* **81**, 800 (2021).
- [63] CMS Collaboration, CMS luminosity measurement for the 2017 data-taking period at $\sqrt{s} = 13$ TeV, CMS Physics Analysis Summary, Report No. CMS-PAS-LUM-17-004, 2018, <https://cds.cern.ch/record/2621960/>.
- [64] CMS Collaboration, CMS luminosity measurement for the 2018 data-taking period at $\sqrt{s} = 13$ TeV, CMS Physics Analysis Summary, Report No. CMS-PAS-LUM-18-002, 2019, <https://cds.cern.ch/record/2676164/>.
- [65] CMS Collaboration, Event generator tunes obtained from underlying event and multiparton scattering measurements, *Eur. Phys. J. C* **76**, 155 (2016).
- [66] CMS Collaboration, Extraction and validation of a new set of CMS *PYTHIA* 8 tunes from underlying-event measurements, *Eur. Phys. J. C* **80**, 4 (2020).
- [67] R. D. Ball *et al.* (NNPDF Collaboration), Parton distributions for the LHC run II, *J. High Energy Phys.* **04** (2015) 040.
- [68] R. D. Ball *et al.* (NNPDF Collaboration), Parton distributions from high-precision collider data, *Eur. Phys. J. C* **77**, 663 (2017).
- [69] CMS Collaboration, Particle-flow reconstruction and global event description with the CMS detector, *J. Instrum.* **12**, P10003 (2017).
- [70] CMS Collaboration, Electron and photon reconstruction and identification with the CMS experiment at the CERN LHC, *J. Instrum.* **16**, P05014 (2021).
- [71] CMS Collaboration, Performance of the CMS muon detector and muon reconstruction with proton-proton collisions at $\sqrt{s} = 13$ TeV, *J. Instrum.* **13**, P06015 (2018).
- [72] CMS Collaboration, Performance of photon reconstruction and identification with the CMS detector in proton-proton collisions at $\sqrt{s} = 8$ TeV, *J. Instrum.* **10**, P08010 (2015).
- [73] M. Cacciari, G. P. Salam, and G. Soyez, The anti- k_T jet clustering algorithm, *J. High Energy Phys.* **04** (2008) 063.
- [74] M. Cacciari, G. P. Salam, and G. Soyez, *FastJet* user manual, *Eur. Phys. J. C* **72**, 1896 (2012).
- [75] CMS Collaboration, Pileup mitigation at CMS in 13 TeV data, *J. Instrum.* **15**, P09018 (2020).
- [76] CMS Collaboration, Jet energy scale and resolution in the CMS experiment in pp collisions at 8 TeV, *J. Instrum.* **12**, P02014 (2017).
- [77] CMS Collaboration, Performance of missing transverse momentum reconstruction in proton-proton collisions at $\sqrt{s} = 13$ TeV using the CMS detector, *J. Instrum.* **14**, P07004 (2019).
- [78] CMS Collaboration, Technical proposal for the Phase-II upgrade of the compact muon solenoid, CMS Technical Proposal, Reports No. CERN-LHCC-2015-010, No. CMS-TDR-15-02, 2015, <http://cds.cern.ch/record/2020886>.
- [79] M. Ester, H.-P. Kriegel, J. Sander, and X. Xu, A density-based algorithm for discovering clusters in large spatial databases with noise, in *Proceedings of 2nd International Conference on Knowledge Discovery and Data Mining (Association for the Advancement of Artificial Intelligence, 1996)*, p. 226, <https://cdn.aaai.org/KDD/1996/KDD96-037.pdf>.
- [80] CMS Collaboration, Identification of b-quark jets with the CMS experiment, *J. Instrum.* **8**, P04013 (2013).
- [81] CMS Collaboration, Identification of heavy-flavour jets with the CMS detector in pp collisions at 13 TeV, *J. Instrum.* **13**, P05011 (2018).
- [82] T. Junk, Confidence level computation for combining searches with small statistics, *Nucl. Instrum. Methods Phys. Res., Sect. A* **434**, 435 (1999).
- [83] A. L. Read, Presentation of search results: The CL_s technique, *J. Phys. G* **28**, 2693 (2002).
- [84] ATLAS and CMS Collaborations, and the LHC Higgs Combination Group, Procedure for the LHC Higgs boson search combination in Summer 2011, Technical Reports No. CMS-NOTE-2011-005, No. ATL-PHYS-PUB-2011-11, 2011, <https://cds.cern.ch/record/1379837>.
- [85] G. Cowan, K. Cranmer, E. Gross, and O. Vitells, Asymptotic formulae for likelihood-based tests of new physics, *Eur. Phys. J. C* **71**, 1554 (2011); **73**, 2501(E) (2013).
- [86] M. Drewes, J. Klarić, and J. López-Pavón, New benchmark models for heavy neutral lepton searches, *Eur. Phys. J. C* **82**, 1176 (2022).

A. Hayrapetyan,¹ A. Tumasyan^{1,b} W. Adam² J. W. Andrejkovic,² T. Bergauer² S. Chatterjee² K. Damanakis² M. Dragicevic² P. S. Hussain² M. Jeitler^{2,c} N. Krammer² A. Li² D. Liko² I. Mikulec² J. Schieck^{2,c} R. Schöfbeck² D. Schwarz² M. Sonawane² S. Templ² W. Waltenberger² C.-E. Wulz^{2,c} M. R. Darwish^{3,d} T. Janssen³ P. Van Mechelen³ E. S. Bols⁴ J. D’Hondt⁴ S. Dansana⁴ A. De Moor⁴ M. Delcourt⁴ H. El Faham⁴ S. Lowette⁴ I. Makarenko⁴ D. Müller⁴ A. R. Sahasransu⁴ S. Tavernier⁴ M. Tytgat^{4,e} S. Van Putte⁴ D. Vannerom⁴ B. Clerbaux⁵ G. De Lentdecker⁵ L. Favart⁵ D. Hohov⁵ J. Jaramillo⁵ A. Khalilzadeh,⁵ K. Lee⁵ M. Mahdavihorrani⁵ A. Malara⁵ S. Paredes⁵ L. Pétré⁵ N. Postiau,⁵ L. Thomas⁵ M. Vanden Bemden⁵ C. Vander Velde⁵ P. Vanlaer⁵ M. De Coen⁶ D. Dobur⁶ Y. Hong⁶ J. Knolle⁶ L. Lambrecht⁶ G. Mestdach,⁶ C. Rendón,⁶ A. Samalan,⁶ K. Skovpen⁶ N. Van Den Bossche⁶ L. Wezenbeek⁶

A. Benecke⁷, G. Bruno⁷, C. Caputo⁷, C. Delaere⁷, I. S. Donertas⁷, A. Giammanco⁷, K. Jaffel⁷, Sa. Jain⁷, V. Lemaître⁷, J. Lidrych⁷, P. Mastrapasqua⁷, K. Mondal⁷, T. T. Tran⁷, S. Wertz⁷, G. A. Alves⁸, E. Coelho⁸, C. Hensel⁸, T. Menezes De Oliveira⁸, A. Moraes⁸, P. Rebello Teles⁸, M. Soeiro⁸, W. L. Aldá Júnior⁹, M. Alves Gallo Pereira⁹, M. Barroso Ferreira Filho⁹, H. Brandao Malbouisson⁹, W. Carvalho⁹, J. Chinellato^{9,f}, E. M. Da Costa⁹, G. G. Da Silveira^{9,g}, D. De Jesus Damiao⁹, S. Fonseca De Souza⁹, J. Martins^{9,h}, C. Mora Herrera⁹, K. Mota Amarilo⁹, L. Mundim⁹, H. Nogima⁹, A. Santoro⁹, A. Sznajder⁹, M. Thiel⁹, A. Vilela Pereira⁹, C. A. Bernardes^{10,g}, L. Calligaris¹⁰, T. R. Fernandez Perez Tomei¹⁰, E. M. Gregores¹⁰, P. G. Mercadante¹⁰, S. F. Novaes¹⁰, B. Orzari¹⁰, Sandra S. Padula¹⁰, A. Aleksandrov¹¹, G. Antchev¹¹, R. Hadjiiska¹¹, P. Iaydjiev¹¹, M. Misheva¹¹, M. Shopova¹¹, G. Sultanov¹¹, A. Dimitrov¹², L. Litov¹², B. Pavlov¹², P. Petkov¹², A. Petrov¹², E. Shumka¹², S. Keshri¹³, S. Thakur¹³, T. Cheng¹⁴, Q. Guo¹⁴, T. Javaid¹⁴, L. Yuan¹⁴, Z. Hu¹⁵, J. Liu¹⁵, K. Yi^{15,i,j}, G. M. Chen^{16,k}, H. S. Chen^{16,k}, M. Chen^{16,k}, F. Iemmi¹⁶, C. H. Jiang¹⁶, A. Kapoor^{16,l}, H. Liao¹⁶, Z.-A. Liu^{16,m}, R. Sharma^{16,n}, J. N. Song^{16,m}, J. Tao¹⁶, C. Wang^{16,k}, J. Wang¹⁶, Z. Wang^{16,k}, H. Zhang¹⁶, A. Agapitos¹⁷, Y. Ban¹⁷, A. Levin¹⁷, C. Li¹⁷, Q. Li¹⁷, Y. Mao¹⁷, S. J. Qian¹⁷, X. Sun¹⁷, D. Wang¹⁷, H. Yang¹⁷, L. Zhang¹⁷, C. Zhou¹⁷, Z. You¹⁸, N. Lu¹⁹, G. Bauer^{20,o}, X. Gao^{21,p}, D. Leggat²¹, H. Okawa²¹, Y. Zhang²¹, Z. Lin²², C. Lu²², M. Xiao²², C. Avila²³, D. A. Barbosa Trujillo²³, A. Cabrera²³, C. Florez²³, J. Fraga²³, J. A. Reyes Vega²³, J. Mejia Guisao²⁴, F. Ramirez²⁴, M. Rodriguez²⁴, J. D. Ruiz Alvarez²⁴, D. Giljanovic²⁵, N. Godinovic²⁵, D. Lelas²⁵, A. Sculac²⁵, M. Kovac²⁶, T. Sculac^{26,q}, P. Bargassa²⁷, V. Brigljevic²⁷, B. K. Chitroda²⁷, D. Ferencek²⁷, S. Mishra²⁷, A. Starodumov^{27,r}, T. Susa²⁷, A. Attikis²⁸, K. Christoforou²⁸, S. Konstantinou²⁸, J. Mousa²⁸, C. Nicolaou²⁸, F. Ptochos²⁸, P. A. Razis²⁸, H. Rykaczewski²⁸, H. Saka²⁸, A. Stepennov²⁸, M. Finger²⁹, M. Finger Jr.²⁹, A. Kveton²⁹, E. Ayala³⁰, E. Carrera Jarrin³¹, S. Elgammal^{32,s}, A. Ellithi Kamel^{32,t}, M. Abdullah Al-Mashad³³, M. A. Mahmoud³³, R. K. Dewanjee^{34,u}, K. Ehataht³⁴, M. Kadastik³⁴, T. Lange³⁴, S. Nandan³⁴, C. Nielsen³⁴, J. Pata³⁴, M. Raidal³⁴, L. Tani³⁴, C. Veelken³⁴, H. Kirschenmann³⁵, K. Osterberg³⁵, M. Voutilainen³⁵, S. Bharthuar³⁶, E. Brücken³⁶, F. Garcia³⁶, J. Havukainen³⁶, K. T. S. Kallonen³⁶, R. Kinnunen³⁶, T. Lampén³⁶, K. Lassila-Perini³⁶, S. Lehti³⁶, T. Lindén³⁶, M. Lotti³⁶, L. Martikainen³⁶, M. Myllymäki³⁶, M. m. Rantanen³⁶, H. Siikonen³⁶, E. Tuominen³⁶, J. Tuominiemi³⁶, P. Luukka³⁷, H. Petrow³⁷, T. Tuuva^{37,a}, M. Besancon³⁸, F. Couderc³⁸, M. Dejardin³⁸, D. Denegri³⁸, J. L. Faure³⁸, F. Ferri³⁸, S. Ganjour³⁸, P. Gras³⁸, G. Hamel de Monchenault³⁸, V. Lohezic³⁸, J. Malcles³⁸, J. Rander³⁸, A. Rosowsky³⁸, M. Ö. Sahin³⁸, A. Savoy-Navarro^{38,v}, P. Simkina³⁸, M. Titov³⁸, M. Tornago³⁸, C. Baldenegro Barrera³⁹, F. Beaudette³⁹, A. Buchot Perraguin³⁹, P. Busson³⁹, A. Cappati³⁹, C. Charlot³⁹, F. Damas³⁹, O. Davignon³⁹, A. De Wit³⁹, G. Falmagne³⁹, B. A. Fontana Santos Alves³⁹, S. Ghosh³⁹, A. Gilbert³⁹, R. Granier de Cassagnac³⁹, A. Hakimi³⁹, B. Harikrishnan³⁹, L. Kalipoliti³⁹, G. Liu³⁹, J. Motta³⁹, M. Nguyen³⁹, C. Ochando³⁹, L. Portales³⁹, R. Salerno³⁹, J. B. Sauvan³⁹, Y. Sirois³⁹, A. Tarabini³⁹, E. Vernazza³⁹, A. Zabi³⁹, A. Zghiche³⁹, J.-L. Agram^{40,w}, J. Andrea⁴⁰, D. Appar⁴⁰, D. Bloch⁴⁰, J.-M. Brom⁴⁰, E. C. Chabert⁴⁰, C. Collard⁴⁰, S. Falke⁴⁰, U. Goerlach⁴⁰, C. Grimault⁴⁰, R. Haeberle⁴⁰, A.-C. Le Bihan⁴⁰, M. Meena⁴⁰, G. Saha⁴⁰, M. A. Sessini⁴⁰, P. Van Hove⁴⁰, S. Beauceron⁴¹, B. Blancon⁴¹, G. Boudoul⁴¹, N. Chanon⁴¹, J. Choi⁴¹, D. Contardo⁴¹, P. Depasse⁴¹, C. Dozen^{41,x}, H. El Mamouni⁴¹, J. Fay⁴¹, S. Gascon⁴¹, M. Gouzevitch⁴¹, C. Greenberg⁴¹, G. Grenier⁴¹, B. Ille⁴¹, I. B. Laktineh⁴¹, M. Lethuillier⁴¹, L. Mirabito⁴¹, S. Perries⁴¹, A. Purohit⁴¹, M. Vander Donckt⁴¹, P. Verdier⁴¹, J. Xiao⁴¹, I. Lomidze⁴², T. Toriashvili^{42,y}, Z. Tsamalaidze^{42,r}, V. Botta⁴³, L. Feld⁴³, K. Klein⁴³, M. Lipinski⁴³, D. Meuser⁴³, A. Pauls⁴³, N. Röwert⁴³, M. Teroerde⁴³, S. Diekmann⁴⁴, A. Dodonova⁴⁴, N. Eich⁴⁴, D. Eliseev⁴⁴, F. Engelke⁴⁴, M. Erdmann⁴⁴, P. Fackeldey⁴⁴, B. Fischer⁴⁴, T. Hebbeker⁴⁴, K. Hoepfner⁴⁴, F. Ivone⁴⁴, A. Jung⁴⁴, M. y. Lee⁴⁴, L. Mastrolorenzo⁴⁴, F. Mausolf⁴⁴, M. Merschmeyer⁴⁴, A. Meyer⁴⁴, S. Mukherjee⁴⁴, D. Noll⁴⁴, A. Novak⁴⁴, F. Nowotny⁴⁴, A. Pozdnyakov⁴⁴, Y. Rath⁴⁴, W. Redjeb⁴⁴, F. Rehm⁴⁴, H. Reithler⁴⁴, U. Sarkar⁴⁴, V. Sarkisovi⁴⁴, A. Schmidt⁴⁴, A. Sharma⁴⁴, J. L. Spah⁴⁴, A. Stein⁴⁴, F. Torres Da Silva De Araujo^{44,z}, L. Vigilante⁴⁴, S. Wiedenbeck⁴⁴, S. Zaleski⁴⁴, C. Dziwok⁴⁵, G. Flügge⁴⁵, W. Haj Ahmad^{45,aa}, T. Kress⁴⁵, A. Nowack⁴⁵, O. Pooth⁴⁵, A. Stahl⁴⁵, T. Ziemons⁴⁵, A. Zotz⁴⁵, H. Aarup Petersen⁴⁶, M. Aldaya Martin⁴⁶, J. Alimena⁴⁶, S. Amoroso⁴⁶, Y. An⁴⁶, S. Baxter⁴⁶, M. Bayatmakou⁴⁶, H. Becerril Gonzalez⁴⁶, O. Behnke⁴⁶, A. Belvedere⁴⁶, S. Bhattacharya⁴⁶, F. Blekman^{46,bb}, K. Borras^{46,cc}, D. Brunner⁴⁶, A. Campbell⁴⁶, A. Cardini⁴⁶, C. Cheng⁴⁶, F. Colombina⁴⁶, S. Consuegra Rodríguez⁴⁶, G. Correia Silva⁴⁶, M. De Silva⁴⁶, G. Eckerlin⁴⁶, D. Eckstein⁴⁶

L. I. Estevez Banos⁴⁶, O. Filatov⁴⁶, E. Gallo^{46,bb}, A. Geiser⁴⁶, A. Giraldo⁴⁶, G. Greau⁴⁶, V. Guglielmi⁴⁶, M. Guthoff⁴⁶, A. Hinzmann⁴⁶, A. Jafari^{46,dd}, L. Jeppe⁴⁶, N. Z. Jomhari⁴⁶, B. Kaech⁴⁶, M. Kasemann⁴⁶, H. Kaveh⁴⁶, C. Kleinwort⁴⁶, R. Kogler⁴⁶, M. Komm⁴⁶, D. Krücker⁴⁶, W. Lange⁴⁶, D. Leyva Pernia⁴⁶, K. Lipka^{46,ee}, W. Lohmann^{46,ff}, R. Mankel⁴⁶, I.-A. Melzer-Pellmann⁴⁶, M. Mendizabal Morentin⁴⁶, J. Metwally⁴⁶, A. B. Meyer⁴⁶, G. Milella⁴⁶, A. Mussgiller⁴⁶, L. P. Nair⁴⁶, A. Nürnberg⁴⁶, Y. Otari⁴⁶, J. Park⁴⁶, D. Pérez Adán⁴⁶, E. Ranken⁴⁶, A. Raspereza⁴⁶, B. Ribeiro Lopes⁴⁶, J. Rübenach⁴⁶, A. Saggio⁴⁶, M. Scham^{46,gg,cc}, S. Schnake^{46,cc}, P. Schütze⁴⁶, C. Schwanenberger^{46,bb}, D. Selivanova⁴⁶, M. Shchedrolosiev⁴⁶, R. E. Sosa Ricardo⁴⁶, D. Stafford⁴⁶, F. Vazzoler⁴⁶, A. Ventura Barroso⁴⁶, R. Walsh⁴⁶, Q. Wang⁴⁶, Y. Wen⁴⁶, K. Wichmann⁴⁶, L. Wiens^{46,cc}, C. Wissing⁴⁶, Y. Yang⁴⁶, A. Zimmermann Castro Santos⁴⁶, A. Albrecht⁴⁷, S. Albrecht⁴⁷, M. Antonello⁴⁷, S. Bein⁴⁷, L. Benato⁴⁷, M. Bonanomi⁴⁷, P. Connor⁴⁷, M. Eich⁴⁷, K. El Morabit⁴⁷, Y. Fischer⁴⁷, A. Fröhlich⁴⁷, C. Garbers⁴⁷, E. Garutti⁴⁷, A. Grohsjean⁴⁷, M. Hajheidari⁴⁷, J. Haller⁴⁷, H. R. Jabusch⁴⁷, G. Kasieczka⁴⁷, P. Keicher⁴⁷, R. Klanner⁴⁷, W. Korcar⁴⁷, T. Kramer⁴⁷, V. Kutzner⁴⁷, F. Labe⁴⁷, J. Lange⁴⁷, A. Lobanov⁴⁷, C. Matthies⁴⁷, A. Mehta⁴⁷, L. Moureaux⁴⁷, M. Mrowietz⁴⁷, A. Nigamova⁴⁷, Y. Nissan⁴⁷, A. Paasch⁴⁷, K. J. Pena Rodriguez⁴⁷, T. Quadfasel⁴⁷, B. Raciti⁴⁷, M. Rieger⁴⁷, D. Savoie⁴⁷, J. Schindler⁴⁷, P. Schleper⁴⁷, M. Schröder⁴⁷, J. Schwandt⁴⁷, M. Sommerhalder⁴⁷, H. Stadio⁴⁷, G. Steinbrück⁴⁷, A. Tews⁴⁷, M. Wolf⁴⁷, S. Brommer⁴⁸, M. Burkart⁴⁸, E. Butz⁴⁸, T. Chwalek⁴⁸, A. Dierlamm⁴⁸, A. Droll⁴⁸, N. Faltermann⁴⁸, M. Giffels⁴⁸, A. Gottmann⁴⁸, F. Hartmann^{48,hh}, R. Hofsaess⁴⁸, M. Horzela⁴⁸, U. Husemann⁴⁸, J. Kieseler⁴⁸, M. Klute⁴⁸, R. Koppenhöfer⁴⁸, J. M. Lawhorn⁴⁸, M. Link⁴⁸, A. Lintuluoto⁴⁸, S. Maier⁴⁸, S. Mitra⁴⁸, M. Mormile⁴⁸, Th. Müller⁴⁸, M. Neukum⁴⁸, M. Oh⁴⁸, M. Presilla⁴⁸, G. Quast⁴⁸, K. Rabbertz⁴⁸, B. Regnery⁴⁸, N. Shadskiy⁴⁸, I. Shvetsov⁴⁸, H. J. Simonis⁴⁸, M. Toms^{48,r}, N. Trevisani⁴⁸, R. Ulrich⁴⁸, J. van der Linden⁴⁸, R. F. Von Cube⁴⁸, M. Wassmer⁴⁸, S. Wieland⁴⁸, F. Wittig⁴⁸, R. Wolf⁴⁸, S. Wunsch⁴⁸, X. Zuo⁴⁸, G. Anagnostou⁴⁹, G. Daskalakis⁴⁹, A. Kyriakis⁴⁹, A. Papadopoulos^{49,hh}, A. Stakia⁴⁹, P. Kontaxakis⁵⁰, G. Melachroinos⁵⁰, A. Panagiotou⁵⁰, I. Papavergou⁵⁰, I. Paraskevas⁵⁰, N. Saoulidou⁵⁰, K. Theofilatos⁵⁰, E. Tziaferi⁵⁰, K. Vellidis⁵⁰, I. Zisopoulos⁵⁰, G. Bakas⁵¹, T. Chatzistavrou⁵¹, G. Karapostoli⁵¹, K. Kousouris⁵¹, I. Papakrivopoulos⁵¹, E. Siamarkou⁵¹, G. Tsiapolitis⁵¹, A. Zacharopoulou⁵¹, K. Adamidis⁵², I. Bestintzanos⁵², I. Evangelou⁵², C. Foudas⁵², P. Gianneios⁵², C. Kamtsikis⁵², P. Katsoulis⁵², P. Kokkas⁵², P. G. Kosmoglou Kioseoglou⁵², N. Manthos⁵², I. Papadopoulos⁵², J. Strologas⁵², M. Bartók^{53,ii}, C. Hajdu⁵³, D. Horvath^{53,ij,kk}, F. Sikler⁵³, V. Veszpremi⁵³, M. Csanád⁵⁴, K. Farkas⁵⁴, M. M. A. Gadallah^{54,ll}, Á. Kadlecik⁵⁴, P. Major⁵⁴, K. Mandal⁵⁴, G. Pásztor⁵⁴, A. J. Rádl^{54,mm}, G. I. Veres⁵⁴, P. Raics⁵⁵, B. Ujvari⁵⁵, G. Zilizi⁵⁵, G. Bencze⁵⁶, S. Czellar⁵⁶, J. Karancsi^{56,ii}, J. Molnar⁵⁶, Z. Szillasi⁵⁶, T. Csorgo^{56,mm}, F. Nemes^{56,mm}, T. Novak⁵⁷, J. Babbar⁵⁸, S. Bansal⁵⁸, S. B. Beri⁵⁸, V. Bhatnagar⁵⁸, G. Chaudhary⁵⁸, S. Chauhan⁵⁸, N. Dhingra^{58,nn}, A. Kaur⁵⁸, A. Kaur⁵⁸, H. Kaur⁵⁸, M. Kaur⁵⁸, S. Kumar⁵⁸, K. Sandeep⁵⁸, T. Sheokand⁵⁸, J. B. Singh⁵⁸, A. Singla⁵⁸, A. Ahmed⁵⁹, A. Bhardwaj⁵⁹, A. Chhetri⁵⁹, B. C. Choudhary⁵⁹, A. Kumar⁵⁹, A. Kumar⁵⁹, M. Naimuddin⁵⁹, K. Ranjan⁵⁹, S. Saumya⁵⁹, S. Baradia⁶⁰, S. Barman^{60,oo}, S. Bhattacharya⁶⁰, S. Dutta⁶⁰, S. Dutta⁶⁰, P. Palit⁶⁰, S. Sarkar⁶⁰, M. M. Ameen⁶¹, P. K. Behera⁶¹, S. C. Behera⁶¹, S. Chatterjee⁶¹, P. Jana⁶¹, P. Kalbhor⁶¹, J. R. Komaragiri^{61,pp}, D. Kumar^{61,pp}, L. Panwar^{61,pp}, P. R. Pujahari⁶¹, N. R. Saha⁶¹, A. Sharma⁶¹, A. K. Sikdar⁶¹, S. Verma⁶¹, S. Dugad⁶², M. Kumar⁶², G. B. Mohanty⁶², P. Suryadevara⁶², A. Bala⁶³, S. Banerjee⁶³, R. M. Chatterjee⁶³, M. Guchait⁶³, Sh. Jain⁶³, S. Karmakar⁶³, S. Kumar⁶³, G. Majumder⁶³, K. Mazumdar⁶³, S. Parolia⁶³, A. Thachayath⁶³, S. Bahinipati^{63,qq}, A. K. Das⁶⁴, C. Kar⁶⁴, D. Maity^{64,rr}, P. Mal⁶⁴, T. Mishra⁶⁴, V. K. Muraleedharan Nair Bindhu^{64,rr}, K. Naskar^{64,rr}, A. Nayak^{64,rr}, P. Sadangi⁶⁴, P. Saha⁶⁴, S. K. Swain⁶⁴, S. Varghese^{64,rr}, D. Vats^{64,rr}, S. Acharya^{65,ss}, A. Alpana⁶⁵, S. Dube⁶⁵, B. Gomber^{65,ss}, B. Kansal⁶⁵, A. Laha⁶⁵, B. Sahu^{65,ss}, S. Sharma⁶⁵, H. Bakhshiansohi^{66,tt}, E. Khazaie^{66,uu}, M. Zeinali^{66,vv}, S. Chenarani^{67,ww}, S. M. Etesami⁶⁷, M. Khakzad⁶⁷, M. Mohammadi Najafabadi⁶⁷, M. Grunewald⁶⁸, M. Abbrescia^{69a,69b}, R. Aly^{69a,69c,xx}, A. Colaleo^{69a,69b}, D. Creanza^{69a,69c}, B. D'Anzi^{69a,69b}, N. De Filippis^{69a,69c}, M. De Palma^{69a,69b}, A. Di Florio^{69a,69c}, W. Elmetenawee^{69a,69b,xx}, L. Fiore^{69a}, G. Iaselli^{69a,69c}, M. Louka^{69a,69b}, G. Maggi^{69a,69c}, M. Maggi^{69a}, I. Margjeka^{69a,69b}, V. Mastrapasqua^{69a,69b}, S. My^{69a,69b}, S. Nuzzo^{69a,69b}, A. Pellecchia^{69a,69b}, A. Pompili^{69a,69b}, G. Pugliese^{69a,69c}, R. Radogna^{69a}, G. Ramirez-Sanchez^{69a,69c}, D. Ramos^{69a}, A. Ranieri^{69a}, L. Silvestris^{69a}, F. M. Simone^{69a,69b}, Ü. Sözbilir^{69a}, A. Stamerra^{69a}, R. Venditti^{69a}, P. Verwilligen^{69a}, A. Zaza^{69a,69b}, G. Abbiendi^{70a}, C. Battilana^{70a,70b}, D. Bonacorsi^{70a,70b}, L. Borgonovi^{70a}

P. Capiluppi^{70a,70b} A. Castro^{70a,70b} F. R. Cavallo^{70a} M. Cuffiani^{70a,70b} G. M. Dallavalle^{70a} T. Diotallevi^{70a,70b}
 F. Fabbri^{70a} A. Fanfani^{70a,70b} D. Fasanella^{70a,70b} P. Giacomelli^{70a} L. Giommi^{70a,70b} C. Grandi^{70a}
 L. Guiducci^{70a,70b} S. Lo Meo^{70a,yy} L. Lunerti^{70a,70b} S. Marcellini^{70a} G. Masetti^{70a} F. L. Navarra^{70a,70b}
 A. Perrotta^{70a} F. Primavera^{70a,70b} A. M. Rossi^{70a,70b} T. Rovelli^{70a,70b} G. P. Siroli^{70a,70b} S. Costa^{71a,71b,zz}
 A. Di Mattia^{71a} R. Potenza^{71a,71b} A. Tricomi^{71a,71b,zz} C. Tuve^{71a,71b} P. Assiouras^{72a} G. Barbagli^{72a}
 G. Bardelli^{72a,72b} B. Camaiani^{72a,72b} A. Cassese^{72a} R. Ceccarelli^{72a} V. Ciulli^{72a,72b} C. Civinini^{72a}
 R. D'Alessandro^{72a,72b} E. Focardi^{72a,72b} T. Kello^{72a} G. Latino^{72a,72b} P. Lenzi^{72a,72b} M. Lizzo^{72a} M. Meschini^{72a}
 S. Paoletti^{72a} A. Papanastassiou^{72a,72b} G. Sguazzoni^{72a} L. Viliani^{72a} L. Benussi⁷³ S. Bianco⁷³ S. Meola^{73,aaa}
 D. Piccolo⁷³ P. Chatagnon^{74a} F. Ferro^{74a} E. Robutti^{74a} S. Tosi^{74a,74b} A. Benaglia^{75a} G. Boldrini^{75a,75b}
 F. Brivio^{75a} F. Cetorelli^{75a} F. De Guio^{75a,75b} M. E. Dinardo^{75a,75b} P. Dini^{75a} S. Gennai^{75a} R. Gerosa^{75a,75b}
 A. Ghezzi^{75a,75b} P. Govoni^{75a,75b} L. Guzzi^{75a} M. T. Lucchini^{75a,75b} M. Malberti^{75a} S. Malvezzi^{75a}
 A. Massironi^{75a} D. Menasce^{75a} L. Moroni^{75a} M. Paganoni^{75a,75b} D. Pedrini^{75a} B. S. Pinolini^{75a}
 S. Ragazzi^{75a,75b} T. Tabarelli de Fatis^{75a,75b} D. Zuolo^{75a} S. Buontempo^{76a} A. Cagnotta^{76a,76b} F. Carnevali^{76a,76b}
 N. Cavallo^{76a,76c} A. De Iorio^{76a,76b} F. Fabozzi^{76a,76c} A. O. M. Iorio^{76a,76b} L. Lista^{76a,76b,bbb} P. Paolucci^{76a,hh}
 B. Rossi^{76a} C. Sciacca^{76a,76b} R. Ardino^{77a} P. Azzi^{77a} N. Bacchetta^{77a,ccc} M. Biasotto^{77a,ddd} P. Bortignon^{77a}
 A. Bragagnolo^{77a,77b} R. Carlin^{77a,77b} P. Checchia^{77a} T. Dorigo^{77a} F. Gasparini^{77a,77b} U. Gasparini^{77a,77b}
 G. Grosso^{77a} E. Lusiani^{77a} M. Margoni^{77a,77b} A. T. Meneguzzo^{77a,77b} M. Migliorini^{77a,77b} J. Pazzini^{77a,77b}
 P. Ronchese^{77a,77b} R. Rossin^{77a,77b} F. Simonetto^{77a,77b} G. Strong^{77a} M. Tosi^{77a,77b} A. Triossi^{77a,77b}
 S. Ventura^{77a} H. Yarar^{77a,77b} M. Zanetti^{77a,77b} P. Zotto^{77a,77b} A. Zucchetta^{77a,77b} G. Zumerle^{77a,77b}
 S. Abu Zeid^{78a,eee} C. Aimè^{78a,78b} A. Braghieri^{78a} S. Calzaferri^{78a} D. Fiorina^{78a} P. Montagna^{78a,78b} V. Re^{78a}
 C. Riccardi^{78a,78b} P. Salvini^{78a} I. Vai^{78a,78b} P. Vitulo^{78a,78b} S. Ajmal^{79a,79b} P. Asenov^{79a,fff} G. M. Bilei^{79a}
 D. Ciangottini^{79a,79b} L. Fanò^{79a,79b} M. Magherini^{79a,79b} G. Mantovani^{79a,79b} V. Mariani^{79a,79b} M. Menichelli^{79a}
 F. Moscatelli^{79a,fff} A. Rossi^{79a,79b} A. Santocchia^{79a,79b} D. Spiga^{79a} T. Tedeschi^{79a,79b} P. Azzurri^{80a}
 G. Bagliesi^{80a} R. Bhattacharya^{80a} L. Bianchini^{80a,80b} T. Boccali^{80a} E. Bossini^{80a} D. Bruschini^{80a,80c}
 R. Castaldi^{80a} M. A. Ciocci^{80a,80b} M. Cipriani^{80a,80b} V. D'Amante^{80a,80d} R. Dell'Orso^{80a} S. Donato^{80a}
 A. Giassi^{80a} F. Ligabue^{80a,80c} D. Matos Figueiredo^{80a} A. Messineo^{80a,80b} M. Musich^{80a,80b} F. Palla^{80a}
 A. Rizzi^{80a,80b} G. Rolandi^{80a,80c} S. Roy Chowdhury^{80a} T. Sarkar^{80a} A. Scribano^{80a} P. Spagnolo^{80a}
 R. Tenchini^{80a} G. Tonelli^{80a,80b} N. Turini^{80a,80d} A. Venturi^{80a} P. G. Verdini^{80a} P. Barria^{81a} M. Campana^{81a,81b}
 F. Cavallari^{81a} L. Cunqueiro Mendez^{81a,81b} D. Del Re^{81a,81b} E. Di Marco^{81a} M. Diemoz^{81a} F. Errico^{81a,81b}
 E. Longo^{81a,81b} P. Meridiani^{81a} J. Mijuskovic^{81a,81b} G. Organtini^{81a,81b} F. Pandolfi^{81a} R. Paramatti^{81a,81b}
 C. Quaranta^{81a,81b} S. Rahatlou^{81a,81b} C. Rovelli^{81a} F. Santanastasio^{81a,81b} L. Soffi^{81a} N. Amapane^{82a,82b}
 R. Arcidiacono^{82a,82c} S. Argiro^{82a,82b} M. Arneodo^{82a,82c} N. Bartosik^{82a} R. Bellan^{82a,82b} A. Bellora^{82a,82b}
 C. Biino^{82a} N. Cartiglia^{82a} M. Costa^{82a,82b} R. Covarelli^{82a,82b} N. Demaria^{82a} L. Finco^{82a} M. Grippo^{82a,82b}
 B. Kiani^{82a,82b} F. Legger^{82a} F. Luongo^{82a,82b} C. Mariotti^{82a} S. Maselli^{82a} A. Mecca^{82a,82b} E. Migliore^{82a,82b}
 M. Monteno^{82a} R. Mulargia^{82a} M. M. Obertino^{82a,82b} G. Ortona^{82a} L. Pacher^{82a,82b} N. Pastrone^{82a}
 M. Pelliccioni^{82a} M. Ruspa^{82a,82c} F. Siviero^{82a,82b} V. Sola^{82a,82b} A. Solano^{82a,82b} A. Staiano^{82a}
 C. Tarricone^{82a,82b} D. Trocino^{82a} G. Umoret^{82a,82b} E. Vlasov^{82a,82b} S. Belforte^{83a} V. Candelise^{83a,83b}
 M. Casarsa^{83a} F. Cossutti^{83a} K. De Leo^{83a,83b} G. Della Ricca^{83a,83b} S. Dogra⁸⁴ J. Hong⁸⁴ C. Huh⁸⁴
 B. Kim⁸⁴ D. H. Kim⁸⁴ J. Kim⁸⁴ H. Lee⁸⁴ S. W. Lee⁸⁴ C. S. Moon⁸⁴ Y. D. Oh⁸⁴ M. S. Ryu⁸⁴
 S. Sekmen⁸⁴ Y. C. Yang⁸⁴ M. S. Kim⁸⁵ G. Bak⁸⁶ P. Gwak⁸⁶ H. Kim⁸⁶ D. H. Moon⁸⁶ E. Asilar⁸⁷
 D. Kim⁸⁷ T. J. Kim⁸⁷ J. A. Merlin⁸⁷ S. Choi⁸⁸ S. Han⁸⁸ B. Hong⁸⁸ K. Lee⁸⁸ K. S. Lee⁸⁸ S. Lee⁸⁸ J. Park⁸⁸
 S. K. Park⁸⁸ J. Yoo⁸⁸ J. Goh⁸⁹ S. Yang⁸⁹ H. S. Kim⁹⁰ Y. Kim⁹⁰ S. Lee⁹⁰ J. Almond⁹¹ J. H. Bhyun⁹¹ J. Choi⁹¹
 W. Jun⁹¹ J. Kim⁹¹ J. S. Kim⁹¹ S. Ko⁹¹ H. Kwon⁹¹ H. Lee⁹¹ J. Lee⁹¹ J. Lee⁹¹ B. H. Oh⁹¹ S. B. Oh⁹¹
 H. Seo⁹¹ U. K. Yang⁹¹ I. Yoon⁹¹ W. Jang⁹² D. Y. Kang⁹² Y. Kang⁹² S. Kim⁹² B. Ko⁹² J. S. H. Lee⁹²
 Y. Lee⁹² I. C. Park⁹² Y. Roh⁹² I. J. Watson⁹² S. Ha⁹³ H. D. Yoo⁹³ M. Choi⁹⁴ M. R. Kim⁹⁴ H. Lee⁹⁴
 Y. Lee⁹⁴ I. Yu⁹⁴ T. Beyrouthy⁹⁵ Y. Maghrbi⁹⁵ K. Dreimanis⁹⁶ A. Gaile⁹⁶ G. Pikurs⁹⁶ A. Potrebko⁹⁶
 M. Seidel⁹⁶ V. Veckalns^{96,ggg} N. R. Strautnieks⁹⁷ M. Ambrozas⁹⁸ A. Juodagalvis⁹⁸ A. Rinkevicius⁹⁸
 G. Tamulaitis⁹⁸ N. Bin Norjoharuddeen⁹⁹ I. Yusuff^{99,hhh} Z. Zolkapli⁹⁹ J. F. Benitez¹⁰⁰
 A. Castaneda Hernandez¹⁰⁰ H. A. Encinas Acosta¹⁰⁰ L. G. Gallegos Maríñez¹⁰⁰ M. León Coello¹⁰⁰

J. A. Murillo Quijada¹⁰⁰, A. Sehrawat¹⁰⁰, L. Valencia Palomo¹⁰⁰, G. Ayala¹⁰¹, H. Castilla-Valdez¹⁰¹,
 E. De La Cruz-Burelo¹⁰¹, I. Heredia-De La Cruz^{101,iii}, R. Lopez-Fernandez¹⁰¹, C. A. Mondragon Herrera¹⁰¹,
 A. Sánchez Hernández¹⁰¹, C. Oropeza Barrera¹⁰², M. Ramírez García¹⁰², I. Bautista¹⁰³, I. Pedraza¹⁰³,
 H. A. Salazar Ibarguen¹⁰³, C. Uribe Estrada¹⁰³, I. Bujanja¹⁰⁴, N. Raicevic¹⁰⁴, P. H. Butler¹⁰⁵, A. Ahmad¹⁰⁶,
 M. I. Asghar¹⁰⁶, A. Awais¹⁰⁶, M. I. M. Awan¹⁰⁶, H. R. Hoorani¹⁰⁶, W. A. Khan¹⁰⁶, V. Avati¹⁰⁷, L. Grzanka¹⁰⁷,
 M. Malawski¹⁰⁷, H. Bialkowska¹⁰⁸, M. Bluj¹⁰⁸, B. Boimska¹⁰⁸, M. Górski¹⁰⁸, M. Kazana¹⁰⁸, M. Szleper¹⁰⁸,
 P. Zalewski¹⁰⁸, K. Bunkowski¹⁰⁹, K. Doroba¹⁰⁹, A. Kalinowski¹⁰⁹, M. Konecki¹⁰⁹, J. Krolikowski¹⁰⁹,
 A. Muhammad¹⁰⁹, K. Pozniak¹¹⁰, W. Zabolotny¹¹⁰, M. Araujo¹¹¹, D. Bastos¹¹¹, C. Beirão Da Cruz E Silva¹¹¹,
 A. Boletti¹¹¹, M. Bozzo¹¹¹, T. Camporesi¹¹¹, G. Da Molin¹¹¹, P. Faccioli¹¹¹, M. Gallinaro¹¹¹, J. Hollar¹¹¹,
 N. Leonardo¹¹¹, T. Niknejad¹¹¹, A. Petrilli¹¹¹, M. Pisano¹¹¹, J. Seixas¹¹¹, J. Varela¹¹¹, J. W. Wulff¹¹¹, P. Adzic¹¹²,
 P. Milenovic¹¹², M. Dordevic¹¹³, J. Milosevic¹¹³, V. Rekovic¹¹³, M. Aguilar-Benitez¹¹⁴, J. Alcaraz Maestre¹¹⁴,
 Cristina F. Bedoya¹¹⁴, M. Cepeda¹¹⁴, M. Cerrada¹¹⁴, N. Colino¹¹⁴, B. De La Cruz¹¹⁴, A. Delgado Peris¹¹⁴,
 A. Escalante Del Valle¹¹⁴, D. Fernández Del Val¹¹⁴, J. P. Fernández Ramos¹¹⁴, J. Flix¹¹⁴, M. C. Fouz¹¹⁴,
 O. Gonzalez Lopez¹¹⁴, S. Goy Lopez¹¹⁴, J. M. Hernandez¹¹⁴, M. I. Josa¹¹⁴, D. Moran¹¹⁴, C. M. Morcillo Perez¹¹⁴,
 Á. Navarro Tobar¹¹⁴, C. Perez Dengra¹¹⁴, A. Pérez-Calero Yzquierdo¹¹⁴, J. Puerta Pelayo¹¹⁴, I. Redondo¹¹⁴,
 D. D. Redondo Ferrero¹¹⁴, L. Romero¹¹⁴, S. Sánchez Navas¹¹⁴, L. Urda Gómez¹¹⁴, J. Vazquez Escobar¹¹⁴,
 C. Willmott¹¹⁴, J. F. de Trocóniz¹¹⁵, B. Alvarez Gonzalez¹¹⁶, J. Cuevas¹¹⁶, J. Fernandez Menendez¹¹⁶,
 S. Folgueras¹¹⁶, I. Gonzalez Caballero¹¹⁶, J. R. González Fernández¹¹⁶, E. Palencia Cortezon¹¹⁶,
 C. Ramón Álvarez¹¹⁶, V. Rodríguez Bouza¹¹⁶, A. Soto Rodríguez¹¹⁶, A. Trapote¹¹⁶, C. Vico Villalba¹¹⁶,
 P. Vischia¹¹⁶, S. Bhowmik¹¹⁷, S. Blanco Fernández¹¹⁷, J. A. Brochero Cifuentes¹¹⁷, I. J. Cabrillo¹¹⁷,
 A. Calderon¹¹⁷, J. Duarte Campderros¹¹⁷, M. Fernandez¹¹⁷, G. Gomez¹¹⁷, C. Lasasa García¹¹⁷,
 C. Martinez Rivero¹¹⁷, P. Martinez Ruiz del Arbol¹¹⁷, F. Matorras¹¹⁷, P. Matorras Cuevas¹¹⁷,
 E. Navarrete Ramos¹¹⁷, J. Piedra Gomez¹¹⁷, L. Scodellaro¹¹⁷, I. Vila¹¹⁷, J. M. Vizan Garcia¹¹⁷,
 M. K. Jayananda¹¹⁸, B. Kailasapathy^{118,jjj}, D. U. J. Sonnadara¹¹⁸, D. D. C. Wickramarathna¹¹⁸,
 W. G. D. Dharmaratna^{119,kkk}, K. Liyanage¹¹⁹, N. Perera¹¹⁹, N. Wickramage¹¹⁹, D. Abbaneo¹²⁰, C. Amendola¹²⁰,
 E. Auffray¹²⁰, G. Auzinger¹²⁰, J. Baechler¹²⁰, D. Barney¹²⁰, A. Bermúdez Martínez¹²⁰, M. Bianco¹²⁰, B. Bilin¹²⁰,
 A. A. Bin Anuar¹²⁰, A. Bocci¹²⁰, E. Brondolin¹²⁰, C. Caillol¹²⁰, G. Cerminara¹²⁰, N. Chernyavskaya¹²⁰,
 D. d'Enterria¹²⁰, A. Dabrowski¹²⁰, A. David¹²⁰, A. De Roeck¹²⁰, M. M. Defranchis¹²⁰, M. Deile¹²⁰,
 M. Dobson¹²⁰, F. Fallavollita^{120,lll}, L. Forthomme¹²⁰, G. Franzoni¹²⁰, W. Funk¹²⁰, S. Giani¹²⁰, D. Gigi¹²⁰, K. Gill¹²⁰,
 F. Gleze¹²⁰, L. Gouskos¹²⁰, M. Haranko¹²⁰, J. Hegeman¹²⁰, B. Huber¹²⁰, V. Innocente¹²⁰, T. James¹²⁰,
 P. Janot¹²⁰, S. Laurila¹²⁰, P. Lecoq¹²⁰, E. Leutgeb¹²⁰, C. Lourenço¹²⁰, B. Maier¹²⁰, L. Malgeri¹²⁰,
 M. Mannelli¹²⁰, A. C. Marini¹²⁰, M. Matthewman¹²⁰, F. Meijers¹²⁰, S. Mersi¹²⁰, E. Meschi¹²⁰, V. Milosevic¹²⁰,
 F. Monti¹²⁰, F. Moortgat¹²⁰, M. Mulders¹²⁰, I. Neutelings¹²⁰, S. Orfanelli¹²⁰, F. Pantaleo¹²⁰, G. Petrucciani¹²⁰,
 A. Pfeiffer¹²⁰, M. Pierini¹²⁰, D. Piparo¹²⁰, H. Qu¹²⁰, D. Rabady¹²⁰, G. Reales Gutiérrez¹²⁰, M. Rovere¹²⁰,
 H. Sakulin¹²⁰, S. Scarfi¹²⁰, C. Schwick¹²⁰, M. Selvaggi¹²⁰, A. Sharma¹²⁰, K. Shchelina¹²⁰, P. Silva¹²⁰,
 P. Sphicas^{120,mmm}, A. G. Stahl Leitner¹²⁰, A. Steen¹²⁰, S. Summers¹²⁰, D. Treille¹²⁰, P. Tropea¹²⁰, A. Tsirou¹²⁰,
 D. Walter¹²⁰, J. Wanczyk^{120,nnn}, S. Wuchterl¹²⁰, P. Zehetner¹²⁰, P. Zejdl¹²⁰, W. D. Zeuner¹²⁰, T. Bevilacqua^{121,ooo},
 L. Caminada^{121,ooo}, A. Ebrahimi¹²¹, W. Erdmann¹²¹, R. Horisberger¹²¹, Q. Ingram¹²¹, H. C. Kaestli¹²¹,
 D. Kotlinski¹²¹, C. Lange¹²¹, M. Missiroli^{121,ooo}, L. Noehte^{121,ooo}, T. Rohe¹²¹, T. K. Aarrestad¹²²,
 K. Androsov^{122,nnn}, M. Backhaus¹²², A. Calandri¹²², C. Cazzaniga¹²², K. Datta¹²², A. De Cosa¹²²,
 G. Dissertori¹²², M. Dittmar¹²², M. Donegà¹²², F. Eble¹²², M. Galli¹²², K. Gedia¹²², F. Glessgen¹²², C. Grab¹²²,
 D. Hits¹²², W. Luster mann¹²², A.-M. Lyon¹²², R. A. Manzoni¹²², M. Marchegiani¹²², L. Marchese¹²²,
 C. Martin Perez¹²², A. Mascellani^{122,nnn}, F. Nessi-Tedaldi¹²², F. Pauss¹²², V. Perovic¹²², S. Pigazzini¹²²,
 M. Reichmann¹²², C. Reissel¹²², T. Reitenspiess¹²², B. Ristic¹²², F. Riti¹²², D. Ruini¹²², D. A. Sanz Becerra¹²²,
 R. Seidita¹²², J. Steggemann^{122,nnn}, D. Valsecchi¹²², R. Wallny¹²², C. Amsler^{123,ppp}, P. Bärttschi¹²³, C. Botta¹²³,
 D. Brzhechko¹²³, M. F. Canelli¹²³, K. Cormier¹²³, R. Del Burgo¹²³, J. K. Heikkilä¹²³, M. Huwiler¹²³, W. Jin¹²³,
 A. Jofrehei¹²³, B. Kilminster¹²³, S. Leontsinis¹²³, S. P. Liechti¹²³, A. Macchiolo¹²³, P. Meiring¹²³,
 V. M. Mikuni¹²³, U. Molinatti¹²³, A. Reimers¹²³, P. Robmann¹²³, S. Sanchez Cruz¹²³, K. Schweiger¹²³,
 M. Senger¹²³, Y. Takahashi¹²³, R. Tramontano¹²³, C. Adloff^{124,qqq}, D. Bhowmik¹²⁴, C. M. Kuo¹²⁴, W. Lin¹²⁴

P. K. Rout¹²⁴, P. C. Tiwari^{124,pp}, S. S. Yu¹²⁴, L. Ceard¹²⁵, Y. Chao¹²⁵, K. F. Chen¹²⁵, P. s. Chen¹²⁵, Z. g. Chen¹²⁵, W.-S. Hou¹²⁵, T. h. Hsu¹²⁵, Y. w. Kao¹²⁵, R. Khurana¹²⁵, G. Kole¹²⁵, Y. y. Li¹²⁵, R.-S. Lu¹²⁵, E. Paganis¹²⁵, X. f. Su¹²⁵, J. Thomas-Wilsker¹²⁵, L. s. Tsai¹²⁵, H. y. Wu¹²⁵, E. Yazgan¹²⁵, C. Asawatangtrakuldee¹²⁶, N. Srimanobhas¹²⁶, V. Wachirapusanand¹²⁶, D. Agyel¹²⁷, F. Boran¹²⁷, Z. S. Demiroglu¹²⁷, F. Dolek¹²⁷, I. Dumanoglu^{127,rr}, E. Eskut¹²⁷, Y. Guler^{127,sss}, E. Gurpinar Guler^{127,sss}, C. Isik¹²⁷, O. Kara¹²⁷, A. Kayis Topaksu¹²⁷, U. Kiminsu¹²⁷, G. Onengut¹²⁷, K. Ozdemir^{127,ttt}, A. Polatoz¹²⁷, B. Tali^{127,uuu}, U. G. Tok¹²⁷, S. Turkcapar¹²⁷, E. Uslan¹²⁷, I. S. Zorbakir¹²⁷, M. Yalvac^{128,vvv}, B. Akgun¹²⁹, I. O. Atakisi¹²⁹, E. Gülmez¹²⁹, M. Kaya^{129,www}, O. Kaya^{129,xxx}, S. Tekten^{129,yyy}, A. Cakir¹³⁰, K. Cankocak^{130,rrr,zzz}, Y. Komurcu¹³⁰, S. Sen^{130,aaaa}, O. Aydilek¹³¹, S. Cerci^{131,uuu}, V. Epshteyn¹³¹, B. Haciasahinoglu¹³¹, I. Hos^{131,bbbb}, B. Kaynak¹³¹, S. Ozkorucuklu¹³¹, O. Potok¹³¹, H. Sert¹³¹, C. Simsek¹³¹, D. Sunar Cerci^{131,uuu}, C. Zorbilmez¹³¹, B. Isildak^{132,cccc}, A. Boyaryntsev¹³³, B. Grynyov¹³³, L. Levchuk¹³⁴, D. Anthony¹³⁵, J. J. Brooke¹³⁵, A. Bundock¹³⁵, F. Bury¹³⁵, E. Clement¹³⁵, D. Cussans¹³⁵, H. Flacher¹³⁵, M. Glowacki¹³⁵, J. Goldstein¹³⁵, H. F. Heath¹³⁵, L. Kreczko¹³⁵, S. Paramesvaran¹³⁵, S. Seif El Nasr-Storey¹³⁵, V. J. Smith¹³⁵, N. Stylianou^{135,ddd}, K. Walkingshaw Pass¹³⁵, R. White¹³⁵, A. H. Ball¹³⁶, K. W. Bell¹³⁶, A. Belyaev^{136,eeee}, C. Brew¹³⁶, R. M. Brown¹³⁶, D. J. A. Cockerill¹³⁶, C. Cooke¹³⁶, K. V. Ellis¹³⁶, K. Harder¹³⁶, S. Harper¹³⁶, M.-L. Holmberg^{136,fff}, J. Linacre¹³⁶, K. Manolopoulos¹³⁶, D. M. Newbold¹³⁶, E. Olaiya¹³⁶, D. Petyt¹³⁶, T. Reis¹³⁶, G. Salvi¹³⁶, T. Schuh¹³⁶, C. H. Shepherd-Themistocleous¹³⁶, I. R. Tomalin¹³⁶, T. Williams¹³⁶, R. Bainbridge¹³⁷, P. Bloch¹³⁷, C. E. Brown¹³⁷, O. Buchmuller¹³⁷, V. Cacchio¹³⁷, C. A. Carrillo Montoya¹³⁷, G. S. Chahal^{137,gggg}, D. Colling¹³⁷, J. S. Dancu¹³⁷, I. Das¹³⁷, P. Dauncey¹³⁷, G. Davies¹³⁷, J. Davies¹³⁷, M. Della Negra¹³⁷, S. Fayer¹³⁷, G. Fedi¹³⁷, G. Hall¹³⁷, M. H. Hassanshahi¹³⁷, A. Howard¹³⁷, G. Iles¹³⁷, M. Knight¹³⁷, J. Langford¹³⁷, J. León Holgado¹³⁷, L. Lyons¹³⁷, A.-M. Magnan¹³⁷, S. Malik¹³⁷, A. Martelli¹³⁷, M. Mieskolainen¹³⁷, J. Nash^{137,hhhh}, M. Pesaresi¹³⁷, B. C. Radburn-Smith¹³⁷, A. Richards¹³⁷, A. Rose¹³⁷, C. Seez¹³⁷, R. Shukla¹³⁷, A. Tapper¹³⁷, K. Uchida¹³⁷, G. P. Uttley¹³⁷, L. H. Vage¹³⁷, T. Virdee^{137,hh}, M. Vojinovic¹³⁷, N. Wardle¹³⁷, D. Winterbottom¹³⁷, K. Coldham¹³⁸, J. E. Cole¹³⁸, A. Khan¹³⁸, P. Kyberd¹³⁸, I. D. Reid¹³⁸, S. Abdullin¹³⁹, A. Brinkerhoff¹³⁹, B. Caraway¹³⁹, J. Dittmann¹³⁹, K. Hatakeyama¹³⁹, J. Hiltbrand¹³⁹, A. R. Kanuganti¹³⁹, B. McMaster¹³⁹, M. Saunders¹³⁹, S. Sawant¹³⁹, C. Sutantawibul¹³⁹, J. Wilson¹³⁹, R. Bartek¹⁴⁰, A. Dominguez¹⁴⁰, C. Huerta Escamilla¹⁴⁰, A. E. Simsek¹⁴⁰, R. Uniyal¹⁴⁰, A. M. Vargas Hernandez¹⁴⁰, R. Chudasama¹⁴¹, S. I. Cooper¹⁴¹, S. V. Gleyzer¹⁴¹, C. U. Perez¹⁴¹, P. Rumerio^{141,iiii}, E. Usai¹⁴¹, R. Yi¹⁴¹, A. Akpinar¹⁴², A. Albert¹⁴², D. Arcaro¹⁴², C. Cosby¹⁴², Z. Demiragli¹⁴², C. Erice¹⁴², C. Fangmeier¹⁴², C. Fernandez Madrazo¹⁴², E. Fontanesi¹⁴², D. Gastler¹⁴², F. Golf¹⁴², S. Jeon¹⁴², I. Reed¹⁴², J. Rohlf¹⁴², K. Salyer¹⁴², D. Sperka¹⁴², D. Spitzbart¹⁴², I. Suarez¹⁴², A. Tsatsos¹⁴², S. Yuan¹⁴², A. G. Zecchinelli¹⁴², G. Benelli¹⁴³, X. Coubez^{143,cc}, D. Cutts¹⁴³, M. Hadley¹⁴³, U. Heintz¹⁴³, J. M. Hogan^{143,jjjj}, T. Kwon¹⁴³, G. Landsberg¹⁴³, K. T. Lau¹⁴³, D. Li¹⁴³, J. Luo¹⁴³, S. Mondal¹⁴³, M. Narain^{143,a}, N. Pervan¹⁴³, S. Sagir^{143,kkkk}, F. Simpson¹⁴³, M. Stamenkovic¹⁴³, W. Y. Wong¹⁴³, X. Yan¹⁴³, W. Zhang¹⁴³, S. Abbott¹⁴⁴, J. Bonilla¹⁴⁴, C. Brainerd¹⁴⁴, R. Breedon¹⁴⁴, M. Calderon De La Barca Sanchez¹⁴⁴, M. Chertok¹⁴⁴, M. Citron¹⁴⁴, J. Conway¹⁴⁴, P. T. Cox¹⁴⁴, R. Erbacher¹⁴⁴, F. Jensen¹⁴⁴, O. Kukral¹⁴⁴, G. Mocellin¹⁴⁴, M. Mulhearn¹⁴⁴, D. Pellett¹⁴⁴, W. Wei¹⁴⁴, Y. Yao¹⁴⁴, F. Zhang¹⁴⁴, M. Bachtis¹⁴⁵, R. Cousins¹⁴⁵, A. Datta¹⁴⁵, G. Flores Avila¹⁴⁵, J. Hauser¹⁴⁵, M. Ignatenko¹⁴⁵, M. A. Iqbal¹⁴⁵, T. Lam¹⁴⁵, E. Manca¹⁴⁵, A. Nunez Del Prado¹⁴⁵, D. Saltzberg¹⁴⁵, V. Valuev¹⁴⁵, R. Clare¹⁴⁶, J. W. Gary¹⁴⁶, M. Gordon¹⁴⁶, G. Hanson¹⁴⁶, W. Si¹⁴⁶, S. Wimpenny^{146,a}, J. G. Branson¹⁴⁷, S. Cittolin¹⁴⁷, S. Cooperstein¹⁴⁷, D. Diaz¹⁴⁷, J. Duarte¹⁴⁷, L. Giannini¹⁴⁷, J. Guiang¹⁴⁷, R. Kansal¹⁴⁷, V. Krutelyov¹⁴⁷, R. Lee¹⁴⁷, J. Letts¹⁴⁷, M. Masciovecchio¹⁴⁷, F. Mokhtar¹⁴⁷, S. Mukherjee¹⁴⁷, M. Pieri¹⁴⁷, M. Quinnan¹⁴⁷, B. V. Sathia Narayanan¹⁴⁷, V. Sharma¹⁴⁷, M. Tadel¹⁴⁷, E. Vourliotis¹⁴⁷, F. Würthwein¹⁴⁷, Y. Xiang¹⁴⁷, A. Yagil¹⁴⁷, A. Barzdukas¹⁴⁸, L. Brennan¹⁴⁸, C. Campagnari¹⁴⁸, A. Dorsett¹⁴⁸, J. Incandela¹⁴⁸, J. Kim¹⁴⁸, A. J. Li¹⁴⁸, P. Masterson¹⁴⁸, H. Mei¹⁴⁸, M. Oshiro¹⁴⁸, J. Richman¹⁴⁸, U. Sarica¹⁴⁸, R. Schmitz¹⁴⁸, F. Setti¹⁴⁸, J. Sheplock¹⁴⁸, D. Stuart¹⁴⁸, T. Á. Vami¹⁴⁸, S. Wang¹⁴⁸, A. Bornheim¹⁴⁹, O. Cerri¹⁴⁹, A. Latorre¹⁴⁹, J. Mao¹⁴⁹, H. B. Newman¹⁴⁹, M. Spiropulu¹⁴⁹, J. R. Vlimant¹⁴⁹, C. Wang¹⁴⁹, S. Xie¹⁴⁹, R. Y. Zhu¹⁴⁹, J. Alison¹⁵⁰, S. An¹⁵⁰, M. B. Andrews¹⁵⁰, P. Bryant¹⁵⁰, M. Cremonesi¹⁵⁰, V. Dutta¹⁵⁰, T. Ferguson¹⁵⁰, A. Harilal¹⁵⁰, C. Liu¹⁵⁰, T. Mudholkar¹⁵⁰, S. Murthy¹⁵⁰, M. Paulini¹⁵⁰, A. Roberts¹⁵⁰, A. Sanchez¹⁵⁰, W. Terrill¹⁵⁰, J. P. Cumalat¹⁵¹, W. T. Ford¹⁵¹, A. Hassani¹⁵¹, G. Karathanasis¹⁵¹, E. MacDonald¹⁵¹, N. Manganello¹⁵¹, F. Marini¹⁵¹, A. Perloff¹⁵¹, C. Savard¹⁵¹

N. Schonbeck¹⁵¹ K. Stenson¹⁵¹ K. A. Ulmer¹⁵¹ S. R. Wagner¹⁵¹ N. Zipper¹⁵¹ J. Alexander¹⁵²
 S. Bright-Thonney¹⁵² X. Chen¹⁵² D. J. Cranshaw¹⁵² J. Fan¹⁵² X. Fan¹⁵² D. Gadkari¹⁵² S. Hogan¹⁵²
 P. Kotamnives¹⁵² J. Monroy¹⁵² J. R. Patterson¹⁵² J. Reichert¹⁵² M. Reid¹⁵² A. Ryd¹⁵² J. Thom¹⁵²
 P. Wittich¹⁵² R. Zou¹⁵² M. Albrow¹⁵³ M. Alyari¹⁵³ O. Amram¹⁵³ G. Apollinari¹⁵³ A. Apresyan¹⁵³
 L. A. T. Bauerdick¹⁵³ D. Berry¹⁵³ J. Berryhill¹⁵³ P. C. Bhat¹⁵³ K. Burkett¹⁵³ J. N. Butler¹⁵³ A. Canepa¹⁵³
 G. B. Cerati¹⁵³ H. W. K. Cheung¹⁵³ F. Chlebana¹⁵³ G. Cummings¹⁵³ J. Dickinson¹⁵³ I. Dutta¹⁵³
 V. D. Elvira¹⁵³ Y. Feng¹⁵³ J. Freeman¹⁵³ A. Gandrakota¹⁵³ Z. Gece¹⁵³ L. Gray¹⁵³ D. Green¹⁵³
 A. Grummer¹⁵³ S. Grünendahl¹⁵³ D. Guerrero¹⁵³ O. Gutsche¹⁵³ R. M. Harris¹⁵³ R. Heller¹⁵³
 T. C. Herwig¹⁵³ J. Hirschauer¹⁵³ L. Horyn¹⁵³ B. Jayatilaka¹⁵³ S. Jindariani¹⁵³ M. Johnson¹⁵³ U. Joshi¹⁵³
 T. Klijnsma¹⁵³ B. Klima¹⁵³ K. H. M. Kwok¹⁵³ S. Lammel¹⁵³ D. Lincoln¹⁵³ R. Lipton¹⁵³ T. Liu¹⁵³
 C. Madrid¹⁵³ K. Maeshima¹⁵³ C. Mantilla¹⁵³ D. Mason¹⁵³ P. McBride¹⁵³ P. Merkel¹⁵³ S. Mrenna¹⁵³
 S. Nahn¹⁵³ J. Ngadiuba¹⁵³ D. Noonan¹⁵³ V. Papadimitriou¹⁵³ N. Pastika¹⁵³ K. Pedro¹⁵³ C. Pena^{153,III}
 F. Ravera¹⁵³ A. Reinsvold Hall^{153,mmmm} L. Ristori¹⁵³ E. Sexton-Kennedy¹⁵³ N. Smith¹⁵³ A. Soha¹⁵³
 L. Spiegel¹⁵³ S. Stoynev¹⁵³ J. Strait¹⁵³ L. Taylor¹⁵³ S. Tkaczyk¹⁵³ N. V. Tran¹⁵³ L. Uplegger¹⁵³
 E. W. Vaandering¹⁵³ I. Zoi¹⁵³ C. Aruta¹⁵⁴ P. Avery¹⁵⁴ D. Bourilkov¹⁵⁴ L. Cadamuro¹⁵⁴ P. Chang¹⁵⁴
 V. Cherepanov¹⁵⁴ R. D. Field¹⁵⁴ E. Koenig¹⁵⁴ M. Kolosova¹⁵⁴ J. Konigsberg¹⁵⁴ A. Korytov¹⁵⁴ K. H. Lo¹⁵⁴
 K. Matchev¹⁵⁴ N. Menendez¹⁵⁴ G. Mitselmakher¹⁵⁴ K. Mohrman¹⁵⁴ A. Muthirakalayil Madhu¹⁵⁴ N. Rawal¹⁵⁴
 D. Rosenzweig¹⁵⁴ S. Rosenzweig¹⁵⁴ K. Shi¹⁵⁴ J. Wang¹⁵⁴ T. Adams¹⁵⁵ A. Al Kadhim¹⁵⁵ A. Askew¹⁵⁵
 N. Bower¹⁵⁵ R. Habibullah¹⁵⁵ V. Hagopian¹⁵⁵ R. Hashmi¹⁵⁵ R. S. Kim¹⁵⁵ S. Kim¹⁵⁵ T. Kolberg¹⁵⁵
 G. Martinez¹⁵⁵ H. Prosper¹⁵⁵ P. R. Prova¹⁵⁵ O. Viazlo¹⁵⁵ M. Wulansatiti¹⁵⁵ R. Yohay¹⁵⁵ J. Zhang¹⁵⁵
 B. Alsufyani¹⁵⁶ M. M. Baarmand¹⁵⁶ S. Butalla¹⁵⁶ T. Elkafrawy^{156,eeee} M. Hohlmann¹⁵⁶ R. Kumar Verma¹⁵⁶
 M. Rahmani¹⁵⁶ E. Yanes¹⁵⁶ M. R. Adams¹⁵⁷ C. Bennett¹⁵⁷ R. Cavanaugh¹⁵⁷ S. Dittmer¹⁵⁷ R. Escobar Franco¹⁵⁷
 O. Evdokimov¹⁵⁷ C. E. Gerber¹⁵⁷ D. J. Hofman¹⁵⁷ J. h. Lee¹⁵⁷ D. S. Lemos¹⁵⁷ A. H. Merrit¹⁵⁷ C. Mills¹⁵⁷
 S. Nanda¹⁵⁷ G. Oh¹⁵⁷ B. Ozek¹⁵⁷ D. Pilipovic¹⁵⁷ R. Pradhan¹⁵⁷ T. Roy¹⁵⁷ S. Rudrabhatla¹⁵⁷
 M. B. Tonjes¹⁵⁷ N. Varelas¹⁵⁷ X. Wang¹⁵⁷ Z. Ye¹⁵⁷ J. Yoo¹⁵⁷ M. Alhusseini¹⁵⁸ D. Blend¹⁵⁸ K. Dilsiz^{158,nnnn}
 L. Emediato¹⁵⁸ G. Karaman¹⁵⁸ O. K. Köseyan¹⁵⁸ J.-P. Merlo¹⁵⁸ A. Mestvirishvili^{158,oooo} J. Nachtman¹⁵⁸
 O. Neogi¹⁵⁸ H. Ogul^{158,pppp} Y. Onel¹⁵⁸ A. Penzo¹⁵⁸ C. Snyder¹⁵⁸ E. Tiras^{158,qqqq} B. Blumenfeld¹⁵⁹
 L. Corcodilos¹⁵⁹ J. Davis¹⁵⁹ A. V. Gritsan¹⁵⁹ L. Kang¹⁵⁹ S. Kyriacou¹⁵⁹ P. Maksimovic¹⁵⁹ M. Roguljic¹⁵⁹
 J. Roskes¹⁵⁹ S. Sekhar¹⁵⁹ M. Swartz¹⁵⁹ A. Abreu¹⁶⁰ L. F. Alcerro Alcerro¹⁶⁰ J. Anguiano¹⁶⁰ P. Baringer¹⁶⁰
 A. Bean¹⁶⁰ Z. Flowers¹⁶⁰ D. Grove¹⁶⁰ J. King¹⁶⁰ G. Krintiras¹⁶⁰ M. Lazarovits¹⁶⁰ C. Le Mahieu¹⁶⁰
 C. Lindsey¹⁶⁰ J. Marquez¹⁶⁰ N. Minafra¹⁶⁰ M. Murray¹⁶⁰ M. Nickel¹⁶⁰ M. Pitt¹⁶⁰ S. Popescu^{160,rrrr}
 C. Rogan¹⁶⁰ C. Royon¹⁶⁰ R. Salvatico¹⁶⁰ S. Sanders¹⁶⁰ C. Smith¹⁶⁰ Q. Wang¹⁶⁰ G. Wilson¹⁶⁰
 B. Allmond¹⁶¹ A. Ivanov¹⁶¹ K. Kaadze¹⁶¹ A. Kalogeropoulos¹⁶¹ D. Kim¹⁶¹ Y. Maravin¹⁶¹ K. Nam¹⁶¹
 J. Natoli¹⁶¹ D. Roy¹⁶¹ G. Sorrentino¹⁶¹ F. Rebassoo¹⁶² D. Wright¹⁶² A. Baden¹⁶³ A. Belloni¹⁶³
 A. Bethani¹⁶³ Y. M. Chen¹⁶³ S. C. Eno¹⁶³ N. J. Hadley¹⁶³ S. Jabeen¹⁶³ R. G. Kellogg¹⁶³ T. Koeth¹⁶³
 Y. Lai¹⁶³ S. Lascio¹⁶³ A. C. Mignerey¹⁶³ S. Nabili¹⁶³ C. Palmer¹⁶³ C. Papageorgakis¹⁶³ M. M. Paranjpe¹⁶³
 L. Wang¹⁶³ J. Bendavid¹⁶⁴ W. Busza¹⁶⁴ I. A. Cali¹⁶⁴ Y. Chen¹⁶⁴ M. D'Alfonso¹⁶⁴ J. Eysermans¹⁶⁴
 C. Freer¹⁶⁴ G. Gomez-Ceballos¹⁶⁴ M. Goncharov¹⁶⁴ P. Harris¹⁶⁴ D. Hoang¹⁶⁴ D. Kovalskyi¹⁶⁴ J. Krupa¹⁶⁴
 L. Lavezzo¹⁶⁴ Y.-J. Lee¹⁶⁴ K. Long¹⁶⁴ C. Mironov¹⁶⁴ C. Paus¹⁶⁴ D. Rankin¹⁶⁴ C. Roland¹⁶⁴ G. Roland¹⁶⁴
 S. Rothman¹⁶⁴ Z. Shi¹⁶⁴ G. S. F. Stephans¹⁶⁴ J. Wang¹⁶⁴ Z. Wang¹⁶⁴ B. Wyslouch¹⁶⁴ T. J. Yang¹⁶⁴
 B. Crossman¹⁶⁵ B. M. Joshi¹⁶⁵ C. Kapsiak¹⁶⁵ M. Krohn¹⁶⁵ D. Mahon¹⁶⁵ J. Mans¹⁶⁵ B. Marzocchi¹⁶⁵
 S. Pandey¹⁶⁵ M. Revering¹⁶⁵ R. Rusack¹⁶⁵ R. Saradhy¹⁶⁵ N. Schroeder¹⁶⁵ N. Strobbe¹⁶⁵ M. A. Wadud¹⁶⁵
 L. M. Cremaldi¹⁶⁶ K. Bloom¹⁶⁷ M. Bryson¹⁶⁷ D. R. Claes¹⁶⁷ G. Haza¹⁶⁷ J. Hossain¹⁶⁷ C. Joo¹⁶⁷
 I. Kravchenko¹⁶⁷ J. E. Siado¹⁶⁷ W. Tabb¹⁶⁷ A. Vagnerini¹⁶⁷ A. Wightman¹⁶⁷ F. Yan¹⁶⁷ D. Yu¹⁶⁷
 H. Bandyopadhyay¹⁶⁸ L. Hay¹⁶⁸ I. Iashvili¹⁶⁸ A. Kharchilava¹⁶⁸ M. Morris¹⁶⁸ D. Nguyen¹⁶⁸
 S. Rappoccio¹⁶⁸ H. Rejeb Sfar¹⁶⁸ A. Williams¹⁶⁸ G. Alverson¹⁶⁹ E. Barberis¹⁶⁹ J. Dervan¹⁶⁹ Y. Haddad¹⁶⁹
 Y. Han¹⁶⁹ A. Krishna¹⁶⁹ J. Li¹⁶⁹ M. Lu¹⁶⁹ G. Madigan¹⁶⁹ R. Mccarthy¹⁶⁹ D. M. Morse¹⁶⁹ V. Nguyen¹⁶⁹
 T. Orimoto¹⁶⁹ A. Parker¹⁶⁹ L. Skinnari¹⁶⁹ A. Tishelman-Charny¹⁶⁹ B. Wang¹⁶⁹ D. Wood¹⁶⁹
 S. Bhattacharya¹⁷⁰ J. Bueghly¹⁷⁰ Z. Chen¹⁷⁰ K. A. Hahn¹⁷⁰ Y. Liu¹⁷⁰ Y. Miao¹⁷⁰ D. G. Monk¹⁷⁰

M. H. Schmitt¹⁷⁰ A. Taliervo¹⁷⁰ M. Velasco¹⁷⁰ G. Agarwal¹⁷¹ R. Band¹⁷¹ R. Bucci¹⁷¹ S. Castells¹⁷¹
 A. Das¹⁷¹ R. Goldouzian¹⁷¹ M. Hildreth¹⁷¹ K. W. Ho¹⁷¹ K. Hurtado Anampa¹⁷¹ T. Ivanov¹⁷¹ C. Jessop¹⁷¹
 K. Lannon¹⁷¹ J. Lawrence¹⁷¹ N. Loukas¹⁷¹ L. Lutton¹⁷¹ J. Mariano¹⁷¹ N. Marinelli¹⁷¹ I. Mcalister¹⁷¹
 T. McCauley¹⁷¹ C. Mcgrady¹⁷¹ C. Moore¹⁷¹ Y. Musienko^{171,r} H. Nelson¹⁷¹ M. Osherson¹⁷¹ A. Piccinelli¹⁷¹
 R. Ruchti¹⁷¹ A. Townsend¹⁷¹ Y. Wan¹⁷¹ M. Wayne¹⁷¹ H. Yockey¹⁷¹ M. Zarucki¹⁷¹ L. Zygala¹⁷¹ A. Basnet¹⁷²
 B. Bylsma¹⁷² M. Carrigan¹⁷² L. S. Durkin¹⁷² C. Hill¹⁷² M. Joyce¹⁷² M. Nunez Ornelas¹⁷² K. Wei¹⁷²
 B. L. Winer¹⁷² B. R. Yates¹⁷² F. M. Addesa¹⁷³ H. Bouchamaoui¹⁷³ P. Das¹⁷³ G. Dezoort¹⁷³ P. Elmer¹⁷³
 A. Frankenthal¹⁷³ B. Greenberg¹⁷³ N. Haubrich¹⁷³ G. Kopp¹⁷³ S. Kwan¹⁷³ D. Lange¹⁷³ A. Loeliger¹⁷³
 D. Marlow¹⁷³ I. Ojalvo¹⁷³ J. Olsen¹⁷³ A. Shevelev¹⁷³ D. Stickland¹⁷³ C. Tully¹⁷³ S. Malik¹⁷⁴
 A. S. Bakshi¹⁷⁵ V. E. Barnes¹⁷⁵ S. Chandra¹⁷⁵ R. Chawla¹⁷⁵ S. Das¹⁷⁵ A. Gu¹⁷⁵ L. Gutay¹⁷⁵ M. Jones¹⁷⁵
 A. W. Jung¹⁷⁵ D. Kondratyev¹⁷⁵ A. M. Koshy¹⁷⁵ M. Liu¹⁷⁵ G. Negro¹⁷⁵ N. Neumeister¹⁷⁵ G. Paspalaki¹⁷⁵
 S. Piperov¹⁷⁵ V. Scheurer¹⁷⁵ J. F. Schulte¹⁷⁵ M. Stojanovic¹⁷⁵ J. Thieman¹⁷⁵ A. K. Viridi¹⁷⁵ F. Wang¹⁷⁵
 W. Xie¹⁷⁵ J. Dolen¹⁷⁶ N. Parashar¹⁷⁶ A. Pathak¹⁷⁶ D. Acosta¹⁷⁷ A. Baty¹⁷⁷ T. Carnahan¹⁷⁷
 K. M. Ecklund¹⁷⁷ P. J. Fernández Manteca¹⁷⁷ S. Freed¹⁷⁷ P. Gardner¹⁷⁷ F. J. M. Geurts¹⁷⁷ W. Li¹⁷⁷
 O. Miguel Colin¹⁷⁷ B. P. Padley¹⁷⁷ R. Redjimi¹⁷⁷ J. Rotter¹⁷⁷ E. Yigitbasi¹⁷⁷ Y. Zhang¹⁷⁷ A. Bodek¹⁷⁸
 P. de Barbaro¹⁷⁸ R. Demina¹⁷⁸ J. L. Dulemba¹⁷⁸ C. Fallon¹⁷⁸ A. Garcia-Bellido¹⁷⁸ O. Hindrichs¹⁷⁸
 A. Khukhunaishvili¹⁷⁸ N. Parmar¹⁷⁸ P. Parygin^{178,r} E. Popova^{178,r} R. Taus¹⁷⁸ G. P. Van Onsem¹⁷⁸
 K. Goulianos¹⁷⁹ B. Chiarito¹⁸⁰ J. P. Chou¹⁸⁰ Y. Gershtein¹⁸⁰ E. Halkiadakis¹⁸⁰ A. Hart¹⁸⁰ M. Heindl¹⁸⁰
 D. Jaroslawski¹⁸⁰ O. Karacheban^{180,ff} I. Laflotte¹⁸⁰ A. Lath¹⁸⁰ R. Montalvo¹⁸⁰ K. Nash¹⁸⁰ H. Routray¹⁸⁰
 S. Salur¹⁸⁰ S. Schnetzer¹⁸⁰ S. Somalwar¹⁸⁰ R. Stone¹⁸⁰ S. A. Thayil¹⁸⁰ S. Thomas¹⁸⁰ J. Vora¹⁸⁰ H. Wang¹⁸⁰
 H. Acharya¹⁸¹ D. Ally¹⁸¹ A. G. Delannoy¹⁸¹ S. Fiorendi¹⁸¹ S. Higginbotham¹⁸¹ T. Holmes¹⁸¹
 N. Karunaratna¹⁸¹ L. Lee¹⁸¹ E. Nibigira¹⁸¹ S. Spanier¹⁸¹ D. Aebi¹⁸² M. Ahmad¹⁸² O. Bouhali^{182,ssss}
 M. Dalchenko¹⁸² R. Eusebi¹⁸² J. Gilmore¹⁸² T. Huang¹⁸² T. Kamon^{182,tttt} H. Kim¹⁸² S. Luo¹⁸²
 S. Malhotra¹⁸² R. Mueller¹⁸² D. Overton¹⁸² D. Rathjens¹⁸² A. Safonov¹⁸² N. Akchurin¹⁸³ J. Damgov¹⁸³
 V. Hegde¹⁸³ A. Hussain¹⁸³ Y. Kazhykarim¹⁸³ K. Lamichhane¹⁸³ S. W. Lee¹⁸³ A. Mankel¹⁸³ T. Peltola¹⁸³
 I. Volobouev¹⁸³ A. Whitbeck¹⁸³ E. Appelt¹⁸⁴ S. Greene¹⁸⁴ A. Gurrola¹⁸⁴ W. Johns¹⁸⁴
 R. Kunnawalkam Elayavalli¹⁸⁴ A. Melo¹⁸⁴ F. Romeo¹⁸⁴ P. Sheldon¹⁸⁴ S. Tuo¹⁸⁴ J. Velkovska¹⁸⁴
 J. Viinikainen¹⁸⁴ B. Cardwell¹⁸⁵ B. Cox¹⁸⁵ J. Hakala¹⁸⁵ R. Hirosky¹⁸⁵ A. Ledovskoy¹⁸⁵ C. Neu¹⁸⁵
 C. E. Perez Lara¹⁸⁵ P. E. Karchin¹⁸⁶ A. Aravind¹⁸⁷ S. Banerjee¹⁸⁷ K. Black¹⁸⁷ T. Bose¹⁸⁷ S. Dasu¹⁸⁷
 I. De Bruyn¹⁸⁷ P. Everaerts¹⁸⁷ C. Galloni¹⁸⁷ H. He¹⁸⁷ M. Herndon¹⁸⁷ A. Herve¹⁸⁷ C. K. Koraka¹⁸⁷
 A. Lanaro¹⁸⁷ R. Loveless¹⁸⁷ J. Madhusudanan Sreekala¹⁸⁷ A. Mallampalli¹⁸⁷ A. Mohammadi¹⁸⁷ S. Mondal¹⁸⁷
 G. Parida¹⁸⁷ D. Pinna¹⁸⁷ A. Savin¹⁸⁷ V. Shang¹⁸⁷ V. Sharma¹⁸⁷ W. H. Smith¹⁸⁷ D. Teague¹⁸⁷ H. F. Tsoi¹⁸⁷
 W. Vetens¹⁸⁷ A. Warden¹⁸⁷ S. Afanasiev¹⁸⁸ V. Andreev¹⁸⁸ Yu. Andreev¹⁸⁸ T. Aushev¹⁸⁸ M. Azarkin¹⁸⁸
 A. Babaev¹⁸⁸ A. Belyaev¹⁸⁸ V. Blinov^{188,r} E. Boos¹⁸⁸ V. Borshch¹⁸⁸ D. Budkouski¹⁸⁸ V. Bunichev¹⁸⁸
 M. Chadeeva^{188,r} V. Chekhovskiy¹⁸⁸ R. Chistov^{188,r} A. Dermenev¹⁸⁸ T. Dimova^{188,r} D. Druzhkin^{188,uuuu}
 M. Dubinin^{188,uuu} L. Dudko¹⁸⁸ A. Ershov¹⁸⁸ G. Gavrilov¹⁸⁸ V. Gavrilov¹⁸⁸ S. Gninenko¹⁸⁸ V. Golovtsov¹⁸⁸
 N. Golubev¹⁸⁸ I. Golutvin¹⁸⁸ I. Gorbunov¹⁸⁸ A. Gribushin¹⁸⁸ Y. Ivanov¹⁸⁸ V. Kachanov¹⁸⁸ V. Karjavine¹⁸⁸
 A. Karneyeu¹⁸⁸ V. Kim^{188,r} M. Kirakosyan¹⁸⁸ D. Kirpichnikov¹⁸⁸ M. Kirsanov¹⁸⁸ V. Klyukhin¹⁸⁸
 O. Kodolova^{188,vvvv} V. Korenkov¹⁸⁸ A. Kozyrev^{188,r} N. Krasnikov¹⁸⁸ A. Lanev¹⁸⁸ P. Levchenko^{188,wwww}
 N. Lychkovskaya¹⁸⁸ V. Makarenko¹⁸⁸ A. Malakhov¹⁸⁸ V. Matveev^{188,r} V. Murzin¹⁸⁸ A. Nikitenko^{188,xxxx,vvvv}
 S. Obraztsov¹⁸⁸ V. Oreshkin¹⁸⁸ V. Palichik¹⁸⁸ V. Perelygin¹⁸⁸ M. Perfilov¹⁸⁸ S. Petrushanko¹⁸⁸
 S. Polikarpov^{188,r} V. Popov¹⁸⁸ O. Radchenko^{188,r} M. Savina¹⁸⁸ V. Savrin¹⁸⁸ V. Shalaev¹⁸⁸ S. Shmatov¹⁸⁸
 S. Shulha¹⁸⁸ Y. Skovpen^{188,r} S. Slabospitskii¹⁸⁸ V. Smirnov¹⁸⁸ D. Sosnov¹⁸⁸ V. Sulimov¹⁸⁸ E. Tcherniaev¹⁸⁸
 A. Terkulov¹⁸⁸ O. Teryaev¹⁸⁸ I. Tilsova¹⁸⁸ A. Toropin¹⁸⁸ L. Uvarov¹⁸⁸ A. Uzunian¹⁸⁸ A. Vorobyev^{188,a}
 N. Voytishin¹⁸⁸ B. S. Yuldashev^{188,yyyy} A. Zarubin¹⁸⁸ I. Zhizhin¹⁸⁸ and A. Zhokin¹⁸⁸

(CMS Collaboration)

- ¹*Yerevan Physics Institute, Yerevan, Armenia*
²*Institut für Hochenergiephysik, Vienna, Austria*
³*Universiteit Antwerpen, Antwerpen, Belgium*
⁴*Vrije Universiteit Brussel, Brussel, Belgium*
⁵*Université Libre de Bruxelles, Bruxelles, Belgium*
⁶*Ghent University, Ghent, Belgium*
⁷*Université Catholique de Louvain, Louvain-la-Neuve, Belgium*
⁸*Centro Brasileiro de Pesquisas Físicas, Rio de Janeiro, Brazil*
⁹*Universidade do Estado do Rio de Janeiro, Rio de Janeiro, Brazil*
¹⁰*Universidade Estadual Paulista, Universidade Federal do ABC, São Paulo, Brazil*
¹¹*Institute for Nuclear Research and Nuclear Energy, Bulgarian Academy of Sciences, Sofia, Bulgaria*
¹²*University of Sofia, Sofia, Bulgaria*
¹³*Instituto De Alta Investigación, Universidad de Tarapacá, Casilla 7 D, Arica, Chile*
¹⁴*Beihang University, Beijing, China*
¹⁵*Department of Physics, Tsinghua University, Beijing, China*
¹⁶*Institute of High Energy Physics, Beijing, China*
¹⁷*State Key Laboratory of Nuclear Physics and Technology, Peking University, Beijing, China*
¹⁸*Sun Yat-Sen University, Guangzhou, China*
¹⁹*University of Science and Technology of China, Hefei, China*
²⁰*Nanjing Normal University, Nanjing, China*
²¹*Institute of Modern Physics and Key Laboratory of Nuclear Physics and Ion-beam Application (MOE)—Fudan University, Shanghai, China*
²²*Zhejiang University, Hangzhou, Zhejiang, China*
²³*Universidad de Los Andes, Bogota, Colombia*
²⁴*Universidad de Antioquia, Medellin, Colombia*
²⁵*University of Split, Faculty of Electrical Engineering, Mechanical Engineering and Naval Architecture, Split, Croatia*
²⁶*University of Split, Faculty of Science, Split, Croatia*
²⁷*Institute Rudjer Boskovic, Zagreb, Croatia*
²⁸*University of Cyprus, Nicosia, Cyprus*
²⁹*Charles University, Prague, Czech Republic*
³⁰*Escuela Politecnica Nacional, Quito, Ecuador*
³¹*Universidad San Francisco de Quito, Quito, Ecuador*
³²*Academy of Scientific Research and Technology of the Arab Republic of Egypt, Egyptian Network of High Energy Physics, Cairo, Egypt*
³³*Center for High Energy Physics (CHEP-FU), Fayoum University, El-Fayoum, Egypt*
³⁴*National Institute of Chemical Physics and Biophysics, Tallinn, Estonia*
³⁵*Department of Physics, University of Helsinki, Helsinki, Finland*
³⁶*Helsinki Institute of Physics, Helsinki, Finland*
³⁷*Lappeenranta-Lahti University of Technology, Lappeenranta, Finland*
³⁸*IRFU, CEA, Université Paris-Saclay, Gif-sur-Yvette, France*
³⁹*Laboratoire Leprince-Ringuet, CNRS/IN2P3, Ecole Polytechnique, Institut Polytechnique de Paris, Palaiseau, France*
⁴⁰*Université de Strasbourg, CNRS, IPHC UMR 7178, Strasbourg, France*
⁴¹*Institut de Physique des 2 Infinis de Lyon (IP2I), Villeurbanne, France*
⁴²*Georgian Technical University, Tbilisi, Georgia*
⁴³*RWTH Aachen University, I. Physikalisches Institut, Aachen, Germany*
⁴⁴*RWTH Aachen University, III. Physikalisches Institut A, Aachen, Germany*
⁴⁵*RWTH Aachen University, III. Physikalisches Institut B, Aachen, Germany*
⁴⁶*Deutsches Elektronen-Synchrotron, Hamburg, Germany*
⁴⁷*University of Hamburg, Hamburg, Germany*
⁴⁸*Karlsruher Institut fuer Technologie, Karlsruhe, Germany*
⁴⁹*Institute of Nuclear and Particle Physics (INPP), NCSR Demokritos, Aghia Paraskevi, Greece*
⁵⁰*National and Kapodistrian University of Athens, Athens, Greece*
⁵¹*National Technical University of Athens, Athens, Greece*
⁵²*University of Ioánnina, Ioánnina, Greece*
⁵³*HUN-REN Wigner Research Centre for Physics, Budapest, Hungary*
⁵⁴*MTA-ELTE Lendület CMS Particle and Nuclear Physics Group, Eötvös Loránd University, Budapest, Hungary*
⁵⁵*Faculty of Informatics, University of Debrecen, Debrecen, Hungary*

- ⁵⁶*Institute of Nuclear Research ATOMKI, Debrecen, Hungary*
- ⁵⁷*Karoly Robert Campus, MATE Institute of Technology, Gyongyos, Hungary*
- ⁵⁸*Panjab University, Chandigarh, India*
- ⁵⁹*University of Delhi, Delhi, India*
- ⁶⁰*Saha Institute of Nuclear Physics, HBNI, Kolkata, India*
- ⁶¹*Indian Institute of Technology Madras, Madras, India*
- ⁶²*Tata Institute of Fundamental Research-A, Mumbai, India*
- ⁶³*Tata Institute of Fundamental Research-B, Mumbai, India*
- ⁶⁴*National Institute of Science Education and Research, An OCC of Homi Bhabha National Institute, Bhubaneswar, Odisha, India*
- ⁶⁵*Indian Institute of Science Education and Research (IISER), Pune, India*
- ⁶⁶*Isfahan University of Technology, Isfahan, Iran*
- ⁶⁷*Institute for Research in Fundamental Sciences (IPM), Tehran, Iran*
- ⁶⁸*University College Dublin, Dublin, Ireland*
- ^{69a}*INFN Sezione di Bari, Bari, Italy*
- ^{69b}*Università di Bari, Bari, Italy*
- ^{69c}*Politecnico di Bari, Bari, Italy*
- ^{70a}*INFN Sezione di Bologna, Bologna, Italy*
- ^{70b}*Università di Bologna, Bologna, Italy*
- ^{71a}*INFN Sezione di Catania, Catania, Italy*
- ^{71b}*Università di Catania, Catania, Italy*
- ^{72a}*INFN Sezione di Firenze, Firenze, Italy*
- ^{72b}*Università di Firenze, Firenze, Italy*
- ⁷³*INFN Laboratori Nazionali di Frascati, Frascati, Italy*
- ^{74a}*INFN Sezione di Genova, Genova, Italy*
- ^{74b}*Università di Genova, Genova, Italy*
- ^{75a}*INFN Sezione di Milano-Bicocca, Milano, Italy*
- ^{75b}*Università di Milano-Bicocca, Milano, Italy*
- ^{76a}*INFN Sezione di Napoli, Napoli, Italy*
- ^{76b}*Università di Napoli “Federico II,” Napoli, Italy*
- ^{76c}*Università della Basilicata, Potenza, Italy*
- ^{76d}*Scuola Superiore Meridionale (SSM), Napoli, Italy*
- ^{77a}*INFN Sezione di Padova, Padova, Italy*
- ^{77b}*Università di Padova, Padova, Italy*
- ^{77c}*Università di Trento, Trento, Italy*
- ^{78a}*INFN Sezione di Pavia, Pavia, Italy*
- ^{78b}*Università di Pavia, Pavia, Italy*
- ^{79a}*INFN Sezione di Perugia, Perugia, Italy*
- ^{79b}*Università di Perugia, Perugia, Italy*
- ^{80a}*INFN Sezione di Pisa, Pisa, Italy*
- ^{80b}*Università di Pisa, Pisa, Italy*
- ^{80c}*Scuola Normale Superiore di Pisa, Pisa, Italy*
- ^{80d}*Università di Siena, Siena, Italy*
- ^{81a}*INFN Sezione di Roma, Roma, Italy*
- ^{81b}*Sapienza Università di Roma, Roma, Italy*
- ^{82a}*INFN Sezione di Torino, Torino, Italy*
- ^{82b}*Università di Torino, Torino, Italy*
- ^{82c}*Università del Piemonte Orientale, Novara, Italy*
- ^{83a}*INFN Sezione di Trieste, Trieste, Italy*
- ^{83b}*Università di Trieste, Trieste, Italy*
- ⁸⁴*Kyungpook National University, Daegu, Korea*
- ⁸⁵*Department of Mathematics and Physics—GWNNU, Gangneung, Korea*
- ⁸⁶*Chonnam National University, Institute for Universe and Elementary Particles, Kwangju, Korea*
- ⁸⁷*Hanyang University, Seoul, Korea*
- ⁸⁸*Korea University, Seoul, Korea*
- ⁸⁹*Kyung Hee University, Department of Physics, Seoul, Korea*
- ⁹⁰*Sejong University, Seoul, Korea*
- ⁹¹*Seoul National University, Seoul, Korea*
- ⁹²*University of Seoul, Seoul, Korea*
- ⁹³*Yonsei University, Department of Physics, Seoul, Korea*

- ⁹⁴Sungkyunkwan University, Suwon, Korea
- ⁹⁵College of Engineering and Technology, American University of the Middle East (AUM),
Dasman, Kuwait
- ⁹⁶Riga Technical University, Riga, Latvia
- ⁹⁷University of Latvia (LU), Riga, Latvia
- ⁹⁸Vilnius University, Vilnius, Lithuania
- ⁹⁹National Centre for Particle Physics, Universiti Malaya, Kuala Lumpur, Malaysia
- ¹⁰⁰Universidad de Sonora (UNISON), Hermosillo, Mexico
- ¹⁰¹Centro de Investigacion y de Estudios Avanzados del IPN, Mexico City, Mexico
- ¹⁰²Universidad Iberoamericana, Mexico City, Mexico
- ¹⁰³Benemerita Universidad Autonoma de Puebla, Puebla, Mexico
- ¹⁰⁴University of Montenegro, Podgorica, Montenegro
- ¹⁰⁵University of Canterbury, Christchurch, New Zealand
- ¹⁰⁶National Centre for Physics, Quaid-I-Azam University, Islamabad, Pakistan
- ¹⁰⁷AGH University of Krakow, Faculty of Computer Science, Electronics and Telecommunications,
Krakow, Poland
- ¹⁰⁸National Centre for Nuclear Research, Swierk, Poland
- ¹⁰⁹Institute of Experimental Physics, Faculty of Physics, University of Warsaw, Warsaw, Poland
- ¹¹⁰Warsaw University of Technology, Warsaw, Poland
- ¹¹¹Laboratório de Instrumentação e Física Experimental de Partículas, Lisboa, Portugal
- ¹¹²Faculty of Physics, University of Belgrade, Belgrade, Serbia
- ¹¹³VINCA Institute of Nuclear Sciences, University of Belgrade, Belgrade, Serbia
- ¹¹⁴Centro de Investigaciones Energéticas Medioambientales y Tecnológicas (CIEMAT), Madrid, Spain
- ¹¹⁵Universidad Autónoma de Madrid, Madrid, Spain
- ¹¹⁶Universidad de Oviedo, Instituto Universitario de Ciencias y Tecnologías Espaciales de Asturias (ICTEA),
Oviedo, Spain
- ¹¹⁷Instituto de Física de Cantabria (IFCA), CSIC-Universidad de Cantabria, Santander, Spain
- ¹¹⁸University of Colombo, Colombo, Sri Lanka
- ¹¹⁹University of Ruhuna, Department of Physics, Matarara, Sri Lanka
- ¹²⁰CERN, European Organization for Nuclear Research, Geneva, Switzerland
- ¹²¹Paul Scherrer Institut, Villigen, Switzerland
- ¹²²ETH Zurich—Institute for Particle Physics and Astrophysics (IPA), Zurich, Switzerland
- ¹²³Universität Zürich, Zurich, Switzerland
- ¹²⁴National Central University, Chung-Li, Taiwan
- ¹²⁵National Taiwan University (NTU), Taipei, Taiwan
- ¹²⁶High Energy Physics Research Unit, Department of Physics, Faculty of Science,
Chulalongkorn University, Bangkok, Thailand
- ¹²⁷Çukurova University, Physics Department, Science and Art Faculty, Adana, Turkey
- ¹²⁸Middle East Technical University, Physics Department, Ankara, Turkey
- ¹²⁹Bogazici University, Istanbul, Turkey
- ¹³⁰Istanbul Technical University, Istanbul, Turkey
- ¹³¹Istanbul University, Istanbul, Turkey
- ¹³²Yildiz Technical University, Istanbul, Turkey
- ¹³³Institute for Scintillation Materials of National Academy of Science of Ukraine, Kharkiv, Ukraine
- ¹³⁴National Science Centre, Kharkiv Institute of Physics and Technology, Kharkiv, Ukraine
- ¹³⁵University of Bristol, Bristol, United Kingdom
- ¹³⁶Rutherford Appleton Laboratory, Didcot, United Kingdom
- ¹³⁷Imperial College, London, United Kingdom
- ¹³⁸Brunel University, Uxbridge, United Kingdom
- ¹³⁹Baylor University, Waco, Texas, USA
- ¹⁴⁰Catholic University of America, Washington, DC, USA
- ¹⁴¹The University of Alabama, Tuscaloosa, Alabama, USA
- ¹⁴²Boston University, Boston, Massachusetts, USA
- ¹⁴³Brown University, Providence, Rhode Island, USA
- ¹⁴⁴University of California, Davis, Davis, California, USA
- ¹⁴⁵University of California, Los Angeles, California, USA
- ¹⁴⁶University of California, Riverside, Riverside, California, USA
- ¹⁴⁷University of California, San Diego, La Jolla, California, USA
- ¹⁴⁸University of California, Santa Barbara, Department of Physics, Santa Barbara, California, USA
- ¹⁴⁹California Institute of Technology, Pasadena, California, USA

- ¹⁵⁰*Carnegie Mellon University, Pittsburgh, Pennsylvania, USA*
¹⁵¹*University of Colorado Boulder, Boulder, Colorado, USA*
¹⁵²*Cornell University, Ithaca, New York, USA*
¹⁵³*Fermi National Accelerator Laboratory, Batavia, Illinois, USA*
¹⁵⁴*University of Florida, Gainesville, Florida, USA*
¹⁵⁵*Florida State University, Tallahassee, Florida, USA*
¹⁵⁶*Florida Institute of Technology, Melbourne, Florida, USA*
¹⁵⁷*University of Illinois Chicago, Chicago, Illinois, USA*
¹⁵⁸*The University of Iowa, Iowa City, Iowa, USA*
¹⁵⁹*Johns Hopkins University, Baltimore, Maryland, USA*
¹⁶⁰*The University of Kansas, Lawrence, Kansas, USA*
¹⁶¹*Kansas State University, Manhattan, Kansas, USA*
¹⁶²*Lawrence Livermore National Laboratory, Livermore, California, USA*
¹⁶³*University of Maryland, College Park, Maryland, USA*
¹⁶⁴*Massachusetts Institute of Technology, Cambridge, Massachusetts, USA*
¹⁶⁵*University of Minnesota, Minneapolis, Minnesota, USA*
¹⁶⁶*University of Mississippi, Oxford, Mississippi, USA*
¹⁶⁷*University of Nebraska-Lincoln, Lincoln, Nebraska, USA*
¹⁶⁸*State University of New York at Buffalo, Buffalo, New York, USA*
¹⁶⁹*Northeastern University, Boston, Massachusetts, USA*
¹⁷⁰*Northwestern University, Evanston, Illinois, USA*
¹⁷¹*University of Notre Dame, Notre Dame, Indiana, USA*
¹⁷²*The Ohio State University, Columbus, Ohio, USA*
¹⁷³*Princeton University, Princeton, New Jersey, USA*
¹⁷⁴*University of Puerto Rico, Mayaguez, Puerto Rico, USA*
¹⁷⁵*Purdue University, West Lafayette, Indiana, USA*
¹⁷⁶*Purdue University Northwest, Hammond, Indiana, USA*
¹⁷⁷*Rice University, Houston, Texas, USA*
¹⁷⁸*University of Rochester, Rochester, New York, USA*
¹⁷⁹*The Rockefeller University, New York, New York, USA*
¹⁸⁰*Rutgers, The State University of New Jersey, Piscataway, New Jersey, USA*
¹⁸¹*University of Tennessee, Knoxville, Tennessee, USA*
¹⁸²*Texas A&M University, College Station, Texas, USA*
¹⁸³*Texas Tech University, Lubbock, Texas, USA*
¹⁸⁴*Vanderbilt University, Nashville, Tennessee, USA*
¹⁸⁵*University of Virginia, Charlottesville, Virginia, USA*
¹⁸⁶*Wayne State University, Detroit, Michigan, USA*
¹⁸⁷*University of Wisconsin—Madison, Madison, Wisconsin, USA*
¹⁸⁸*An institute or international laboratory covered by a cooperation agreement with CERN*

^aDeceased.

^bAlso at Yerevan State University, Yerevan, Armenia.

^cAlso at TU Wien, Vienna, Austria.

^dAlso at Institute of Basic and Applied Sciences, Faculty of Engineering, Arab Academy for Science, Technology and Maritime Transport, Alexandria, Egypt.

^eAlso at Ghent University, Ghent, Belgium.

^fAlso at Universidade Estadual de Campinas, Campinas, Brazil.

^gAlso at Federal University of Rio Grande do Sul, Porto Alegre, Brazil.

^hAlso at UFMS, Nova Andradina, Brazil.

ⁱAlso at Nanjing Normal University, Nanjing, China.

^jAlso at The University of Iowa, Iowa City, Iowa, USA.

^kAlso at University of Chinese Academy of Sciences, Beijing, China.

^lAlso at China Center of Advanced Science and Technology, Beijing, China.

^mAlso at University of Chinese Academy of Sciences, Beijing, China.

ⁿAlso at China Spallation Neutron Source, Guangdong, China.

^oAlso at Henan Normal University, Xinxiang, China.

^pAlso at Université Libre de Bruxelles, Bruxelles, Belgium.

^qAlso at University of Latvia (LU), Riga, Latvia.

^rAlso at Another institute or international laboratory covered by a cooperation agreement with CERN.

^sAlso at British University in Egypt, Cairo, Egypt.

- ^t Also at Cairo University, Cairo, Egypt.
- ^u Also at Birla Institute of Technology Mesra, Mesra, India.
- ^v Also at Purdue University, West Lafayette, Indiana, USA.
- ^w Also at Université de Haute Alsace, Mulhouse, France.
- ^x Also at Department of Physics, Tsinghua University, Beijing, China.
- ^y Also at Tbilisi State University, Tbilisi, Georgia.
- ^z Also at The University of the State of Amazonas, Manaus, Brazil.
- ^{aa} Also at Erzincan Binali Yildirim University, Erzincan, Turkey.
- ^{bb} Also at University of Hamburg, Hamburg, Germany.
- ^{cc} Also at RWTH Aachen University, III. Physikalisches Institut A, Aachen, Germany.
- ^{dd} Also at Isfahan University of Technology, Isfahan, Iran.
- ^{ee} Also at Bergische University Wuppertal (BUW), Wuppertal, Germany.
- ^{ff} Also at Brandenburg University of Technology, Cottbus, Germany.
- ^{gg} Also at Forschungszentrum Jülich, Juelich, Germany.
- ^{hh} Also at CERN, European Organization for Nuclear Research, Geneva, Switzerland.
- ⁱⁱ Also at Institute of Physics, University of Debrecen, Debrecen, Hungary.
- ^{jj} Also at Institute of Nuclear Research ATOMKI, Debrecen, Hungary.
- ^{kk} Also at Universitatea Babeș-Bolyai—Facultatea de Fizica, Cluj-Napoca, Romania.
- ^{ll} Also at Physics Department, Faculty of Science, Assiut University, Assiut, Egypt.
- ^{mm} Also at HUN-REN Wigner Research Centre for Physics, Budapest, Hungary.
- ⁿⁿ Also at Punjab Agricultural University, Ludhiana, India.
- ^{oo} Also at University of Visva-Bharati, Santiniketan, India.
- ^{pp} Also at Indian Institute of Science (IISc), Bangalore, India.
- ^{qq} Also at IIT Bhubaneswar, Bhubaneswar, India.
- ^{rr} Also at Institute of Physics, Bhubaneswar, India.
- ^{ss} Also at University of Hyderabad, Hyderabad, India.
- ^{tt} Also at Deutsches Elektronen-Synchrotron, Hamburg, Germany.
- ^{uu} Also at Department of Physics, Isfahan University of Technology, Isfahan, Iran.
- ^{vv} Also at Sharif University of Technology, Tehran, Iran.
- ^{ww} Also at Department of Physics, University of Science and Technology of Mazandaran, Behshahr, Iran.
- ^{xx} Also at Helwan University, Cairo, Egypt.
- ^{yy} Also at Italian National Agency for New Technologies, Energy and Sustainable Economic Development, Bologna, Italy.
- ^{zz} Also at Centro Siciliano di Fisica Nucleare e di Struttura Della Materia, Catania, Italy.
- ^{aaa} Also at Università degli Studi Guglielmo Marconi, Roma, Italy.
- ^{bbb} Also at Scuola Superiore Meridionale, Università di Napoli “Federico II,” Napoli, Italy.
- ^{ccc} Also at Fermi National Accelerator Laboratory, Batavia, Illinois, USA.
- ^{ddd} Also at Laboratori Nazionali di Legnaro dell’INFN, Legnaro, Italy.
- ^{eee} Also at Ain Shams University, Cairo, Egypt.
- ^{fff} Also at Consiglio Nazionale delle Ricerche—Istituto Officina dei Materiali, Perugia, Italy.
- ^{ggg} Also at Riga Technical University, Riga, Latvia.
- ^{hhh} Also at Department of Applied Physics, Faculty of Science and Technology, Universiti Kebangsaan Malaysia, Bangi, Malaysia.
- ⁱⁱⁱ Also at Consejo Nacional de Ciencia y Tecnología, Mexico City, Mexico.
- ^{jjj} Also at Trincomalee Campus, Eastern University, Sri Lanka, Nilaveli, Sri Lanka.
- ^{kkk} Also at Saegis Campus, Nugegoda, Sri Lanka.
- ^{lll} Also at INFN Sezione di Pavia, Università di Pavia, Pavia, Italy.
- ^{mmmm} Also at National and Kapodistrian University of Athens, Athens, Greece.
- ⁿⁿⁿ Also at Ecole Polytechnique Fédérale Lausanne, Lausanne, Switzerland.
- ^{ooo} Also at Universität Zürich, Zurich, Switzerland.
- ^{ppp} Also at Stefan Meyer Institute for Subatomic Physics, Vienna, Austria.
- ^{qqq} Also at Laboratoire d’Annecy-le-Vieux de Physique des Particules, IN2P3-CNRS, Annecy-le-Vieux, France.
- ^{rrr} Also at Near East University, Research Center of Experimental Health Science, Mersin, Turkey.
- ^{sss} Also at Konya Technical University, Konya, Turkey.
- ^{ttt} Also at Izmir Bakircay University, Izmir, Turkey.
- ^{uuu} Also at Adiyaman University, Adiyaman, Turkey.
- ^{vvv} Also at Bozok Universitetesi Rektörlüğü, Yozgat, Turkey.
- ^{www} Also at Marmara University, Istanbul, Turkey.
- ^{xxx} Also at Milli Savunma University, Istanbul, Turkey.
- ^{yyy} Also at Kafkas University, Kars, Turkey.
- ^{zzz} Also at Istanbul Okan University, Istanbul, Turkey.
- ^{aaaa} Also at Hacettepe University, Ankara, Turkey.

- bbbb** Also at Istanbul University—Cerrahpasa, Faculty of Engineering, Istanbul, Turkey.
- cccc** Also at Yildiz Technical University, Istanbul, Turkey.
- dddd** Also at Vrije Universiteit Brussel, Brussel, Belgium.
- eeee** Also at School of Physics and Astronomy, University of Southampton, Southampton, United Kingdom.
- ffff** Also at University of Bristol, Bristol, United Kingdom.
- gggg** Also at IPPP Durham University, Durham, United Kingdom.
- hhhh** Also at Monash University, Faculty of Science, Clayton, Australia.
- iiii** Also at Università di Torino, Torino, Italy.
- jjjj** Also at Bethel University, St. Paul, Minnesota, USA.
- kkkk** Also at Karamanoğlu Mehmetbey University, Karaman, Turkey.
- llll** Also at California Institute of Technology, Pasadena, California, USA.
- mmmm** Also at United States Naval Academy, Annapolis, Maryland, USA.
- nnnn** Also at Bingol University, Bingol, Turkey.
- oooo** Also at Georgian Technical University, Tbilisi, Georgia.
- pppp** Also at Sinop University, Sinop, Turkey.
- qqqq** Also at Erciyes University, Kayseri, Turkey.
- rrrr** Also at Horia Hulubei National Institute of Physics and Nuclear Engineering (IFIN-HH), Bucharest, Romania.
- ssss** Also at Texas A&M University at Qatar, Doha, Qatar.
- tttt** Also at Kyungpook National University, Daegu, Korea.
- uuuu** Also at Universiteit Antwerpen, Antwerpen, Belgium.
- vvvv** Also at Yerevan Physics Institute, Yerevan, Armenia.
- wwww** Also at Northeastern University, Boston, Massachusetts, USA.
- xxxx** Also at Imperial College, London, United Kingdom.
- yyyy** Also at Institute of Nuclear Physics of the Uzbekistan Academy of Sciences, Tashkent, Uzbekistan.